

Master Thesis



Czech
Technical
University
in Prague

F3

Faculty of Electrical Engineering
Department of Electroenergetics

Modelling of geomagnetically induced currents in the electric transmission grid operated by ČEPS, a. s.

Bc. Anna Smičková

Supervisor: doc. Mgr. Michal Švanda, Ph.D.; Prof. Dr. ir. Dirk Van Hertem; Dr. ir. Mudar Abedrabbo
August 2021

Acknowledgements

First of all, I would like to thank to my supervisor, Dr. Michal Švanda from Astronomical Institute of Charles University, for providing guidance and feedback for this thesis, providing electric field data. I also want to thank to Dr. Mudar Abedrabbo and Prof. Dirk Van Hertem from KU Leuven for feedback for my thesis and their comments.

Furthermore I would like to thank to Michal Peterka from ČEPS, a. s., for providing transmission grid parameters and to Dr. Pavel Mlejnek for providing the measurements data.

Declaration

I declare that this work is all my own work and I have cited all sources I have used in the bibliography.

Prague, August 12, 2021

Anna Smičková

Prohlašuji, že jsem předloženou práci vypracovala samostatně a že jsem uvedla veškeré použité informační zdroje v souladu s Metodickým pokynem o do-
držování etických principů při přípravě vysokoškolských závěrečných prací.

V Praze, 12. srpna 2021

Anna Smičková

Abstract

In the past, there were several events, that are believed to be associated with Geomagnetically induced currents (GICs), that caused problems with systems on the Earth, for example telegraph systems, buried pipelines or power grids, etc. It is generally believed that these currents lead to increased failure rates of components of the power grid. These effects are well proven for countries at higher latitudes – Scandinavia, USA, Canada, South Africa, etc., where the amplitudes reach up to hundreds of amperes during great solar storms. In the central Europe, such large values of GICs are not expected, but even GICs that are of lower amplitudes can cumulatively cause an increased failure rate.

As the transmission distance is increased and the power transmitted as well, the possible consequences of the GICs might be more serious. As the space weather prediction is almost impossible, it is necessary to investigate, whether the concrete studied system might be affected by possible solar storm. Some countries had already started with studies concerning the GICs and its possible consequences, but in the Czech Republic, this is the first study, modelling the GICs for its transmission system.

This study aims to determine the values of GICs for the event of Halloween storms, that is the most recent solar storm, that significantly affected systems on the Earth surface and to predict possible amplitudes for the event of extreme solar storm. The task of the thesis is to get acquainted in detail with the Lehtinen-Pirjola method of GIC modelling. With the knowledge of this method, data structure of input data for key parameters description of the electrical power network was set and

those data were used by the program that was written in Python for calculation and modelling the time evolution of GICs for entered time period of increased solar activity for specified power grid system. Specifically, it investigates the event of Halloween storm for transmission system in Czech Republic.

The result of the thesis is a program that calculates the GICs for any power network whose key parameters are available in the exact data structure, that is described. The output of this program is automatically generated network topology, time evolution of GICs for each electrical substation in the power grid and also maximum amplitudes of these GICs.

Keywords: Geomagnetic activity, Geomagnetically induced currents, Electric grid, Transmission lines

Supervisor: doc. Mgr. Michal Švanda, Ph.D.; Prof. Dr. ir. Dirk Van Hertem; Dr. ir. Mudar Abedrabbo

Abstrakt

V minulosti bylo zaznamenáno několik událostí, které byly spojovány s Geomagnetickými indukovanými proudy (GIC), které způsobovaly problémy pozemních systémů - telegrafní sítě, ropovody, elektrické přenosové vedení,... Obecně se věří, že tyto proudy vedou ke zvýšení množství poruch komponent elektrických vedení. Tyto efekty jsou velmi dobře prokázány v zemích jako například Skandinávie, USA, Kanada, Jižní Afrika, atd., kde tyto proudy dosahují amplitud několik stovek ampér během velkých solárních bouří. Ve Střední Evropě se takto vysoké hodnoty neočekávají, nicméně i GIC nižších amplitud mohou kumulativně způsobovat poruchovost.

Se zvyšováním přenosových vzdáleností a přenosové schopnosti vedení tyto problémy způsobené GIC mohou být výraznější. Jelikož téměř nelze předpovídat kosmické počasí, je důležité, abychom zkoumali, zda by konkrétní studovaná přenosová soustava mohla být těmito proudy ovlivněna a zda by mohlo dojít k vážnějším problémům při případné geomagnetické bouři. Některé země již se studii GIC a jejich možnými efekty zabývají, pro Českou Republiku je toto první práce, která se zabývá výpočtem GIC pro přenosovou soustavu.

Cílem této práce bylo se seznámit s Lehtinen-Pirjolovou metodou modelování GIC, se znalostí této metody stanovit vhodnou strukturu vstupních dat, se kterou program bude pracovat. Výstupem této práce je program v programovacím jazyce Python, výstupem kterého je časový průběh GIC pro zadaný časový úsek a systém, který zkoumáme. V tomto případě se jedná o výstup pro Halloween-ské bouře v roce 2003 pro napětovou hladinu 400 kV přenosové soustavy České Republiky. Dalším výstupem této práce

jsou předpokládané hodnoty GIC pro událost extrémní bouře, která by mohla případně nastat. Výstup je zobrazen časovým průběhem GIC pro jednotlivé rozvodny v soustavě.

Klíčová slova: Geomagnetická aktivita, Přenosová síť, Geomagnetické indukované proudy

Překlad názvu: Modelování geomagnetických indukovaných proudů v přenosové síti České republiky provozované ČEPS

Contents

1 Introduction	3
2 Literature review	7
2.1 GIC	7
2.1.1 Introduction	7
2.1.2 Space weather	8
2.1.3 Maxwell's equations	9
2.1.4 GIC generation	10
2.1.5 Potential effects on the power grid system components caused by the GICs	12
2.1.6 Events associated with GICs	12
2.1.7 GICs studies in the world . . .	18
3 Czech transmission line	25
3.1 Parameters of the Czech transmission grid	26
4 Lehtinen-Pirjola method of GIC calculation	29
5 Data structure	33
5.1 Coordinates of the transmission line	33
5.2 Grounding resistance of substation	35
5.3 Geoelectric field	35
5.4 Resistivity and length of the transmission lines	36
5.5 Measured data from Mírovka substation	37
6 Model implementation	39
6.1 Data reading	40
6.2 Induced voltages	41
6.3 Ideal-earthing currents	41
6.4 GIC	41
7 Results	43
7.1 Halloween storms	43
7.1.1 Geomagnetic voltage	43
7.1.2 GIC	47
7.2 Geoelectric field of 1 V/km	51
8 Discussion	53
8.1 Effects of the unknown earthing resistances	53
8.2 Validation to measured data . . .	59
9 Conclusions	63
Bibliography	65

Figures

1.1 Share of electricity production in the Czech Republic by source	4	7.4 Geomagnetic voltage for the line V420	46
2.1 The chain of events from a coronal mass ejection (CME) on the Sun to geomagnetically induced currents (GICs) in transmission lines	11	7.5 GIC for Bezděčín substation - Halloween storms 2003	48
2.2 Effect of 3% DC offset in the input voltage on the B-H loop	12	7.6 GIC for Dlouhé Stráně substation - Halloween storms 2003	49
2.3 The sequence of magnetic disturbances experienced in Quebec on 12-14 March 1989	15	7.7 GIC for Mírovka substation - Halloween storms 2003	49
2.4 The location of principal events leading to the blackout	16	7.8 GIC for Tušimice substation - Halloween storms 2003	50
2.5 Measured (red) and calculated (blue) GIC at the TR2 transformer of Vandellòs for the event of 24–25 October 2011	21	7.9 GIC for Hradec Západ substation - Halloween storms 2003	51
2.6 Oil pipelines in Czech Republic .	22	8.1 Calculated GIC for Chvaletice substation for different grounding resistances	54
2.7 Fit between the measured P/S voltage (red) and the computed geoelectric field (black) for the most disturbed period of 29 October 2003	22	8.2 Histogram of differences in results for minimum and average resistance for Chvaletice substation	54
3.1 Schema of the Czech transmission grid	25	8.3 Histogram of differences in results for maximum and average resistance for Chvaletice substation	55
4.1 Scheme of the electrical circuit representing a fictional power grid with six nodes. This scheme demonstrates one of the inputs to the Pirjola-Lehtinen method of GIC calculation	30	8.4 Calculated GIC for Mírovka substation for different grounding resistances	55
5.1 S-JTSK coordinates axes	34	8.5 Histogram of differences in results for for minimum and average resistance for Mírovka substation .	56
5.2 Plotted schema of Czech transmission grid	34	8.6 Histogram of differences in results for for maximum and average resistance for Mírovka substation .	56
5.3 Geoelectric field	36	8.7 Calculated GIC for Neznášov substation for different grounding resistances	57
6.1 The flowchart of the code	40	8.8 Histogram of differences in results for minimum and average resistance for Neznášov substation	57
7.1 Geomagnetic voltage for the line V414	45	8.9 Histogram of differences in results for maximum and average resistance for Neznášov substation	58
7.2 Geomagnetic voltage for the line V415	45	8.10 Comparison of calculated and measured GIC for 27th April 2019	60
7.3 Geomagnetic voltage for the line V416	46	8.11 Comparison of calculated and measured GIC for 28th April 2019	61
		8.12 Comparison of calculated and measured GIC for 29th April 2019	61

8.13 Comparison of calculated and measured GIC for 13th April 2019	62
8.14 Comparison of the measured GIC, modelled GIC in the Mírovka substation over the whole month of April 2019 with the overall geomagnetic activity represented by the K index.	62

Tables

5.1 Grounding resistances of substations that were provided by the ČEPS company	35
7.1 Geomagnetic voltage for all transmission lines	44
7.2 GIC values for Halloween storm 2003	47
7.3 GIC values for geomagnetic field value 1 V/km	52

I. OSOBNÍ A STUDIJNÍ ÚDAJE

Příjmení: **Smičková** Jméno: **Anna** Osobní číslo: **459229**
Fakulta/ústav: **Fakulta elektrotechnická**
Zadávající katedra/ústav: **Katedra elektroenergetiky**
Studijní program: **Elektrotechnika, energetika a management**
Specializace: **Elektroenergetika**

II. ÚDAJE K DIPLOMOVÉ PRÁCI

Název diplomové práce:

Modelování geomagnetických indukovaných proudů v rozvodné síti ČEPS, a.s.

Název diplomové práce anglicky:

Modelling of geomagnetically induced currents in the electric transmission grid operated by ČEPS, a.s.

Pokyny pro vypracování:

1. Řešitel provede rešerši problematiky.
2. Detailně se seznámí s Lehtinenovou-Pirjolovou metodou výpočtu GIC.
3. Navrhne datovou strukturu popisu klíčových parametrů elektrizační sítě, která bude vhodná pro následné automatizované zpracování výpočetním programem.
4. Přířadou komunikací s ČEPS získá potřebné údaje pro 400-kV síť (odpory vedení, zemnicí odpory uzlů, směrování vedení).
5. Vhodnou reprezentací zobrazí topologii sítě jako elektrický obvod.
6. Vytvoří univerzální počítačový program v jazyce dle vlastní volby modelující GIC z geoelektrického pole za znalosti parametrů vedení. Program bude vhodný pro aplikaci na libovolnou topologii rozvodné sítě, jež bude přirozeně vyplývat ze vstupní datové struktury.
7. Aplikuje program na 400-kV elektrizační síť ČEPS ve vybraných obdobích zvýšené geomagnetické aktivity a diskutuje výsledky.

Seznam doporučené literatury:

- * Pirjola, R. (2012). Geomagnetically Induced Currents as Ground Effects of Space Weather, Space Science, Dr. Herman J. Mosquera Cuesta (Ed.), ISBN: 978-953-51-0423-0, InTech, Available from: <http://www.intechopen.com/books/space-science/geomagnetically-induced-currents-a-s-ground-effects-of-space-weather>
- * Boteler, D.H., Pirjola, R.J. (2014). Comparison of methods for modelling geomagnetically induced currents, Ann. Geophys. 32, 1177-1187.
- * Bailey, R.L. et al. (2017). Modelling geomagnetically induced currents in midlatitude Central Europe using a thin-sheet approach. Ann. Geophys. 35, 751–761.
- * Bailey, R.L. et al. (2018). Validating GIC Models With Measurements in Austria: Evaluation of Accuracy and Sensitivity to Input Parameters. Space Weather 16, 887-902.
- * a další aktuální články na téma dle pokynů vedoucího

Jméno a pracoviště vedoucí(ho) diplomové práce:

doc. Mgr. Michal Švanda, Ph. D., Astronomický ústav Univerzity Karlovy

Jméno a pracoviště druhé(ho) vedoucí(ho) nebo konzultanta(ky) diplomové práce:

Datum zadání diplomové práce: **05.10.2020**

Termín odevzdání diplomové práce: **13.08.2021**

Platnost zadání diplomové práce: **30.09.2022**

doc. Mgr. Michal Švanda, Ph. D.
podpis vedoucí(ho) práce

podpis vedoucí(ho) ústavu/katedry

prof. Mgr. Petr Páta, Ph.D.
podpis děkana(ky)

III. PŘEVZETÍ ZADÁNÍ

Diplomantka bere na vědomí, že je povinna vypracovat diplomovou práci samostatně, bez cizí pomoci, s výjimkou poskytnutých konzultací. Seznam použité literatury, jiných pramenů a jmen konzultantů je třeba uvést v diplomové práci.

Datum převzetí zadání

Podpis studentky



Chapter 1

Introduction

One of the most important commodities, that would be very difficult to exist without, is electricity. The need of electricity is clear for all of us and we are almost not able to imagine world without it. Provision of electrical energy to all of us is a complex process, that involves three main stages: generation, transmission, and distribution of electricity.

Electricity is generated in power plants using renewable or non-renewable resources. Most of the power plants use one or more generators, that convert mechanical energy into electrical energy. Most of the generators used in world are electromechanical generators driven by heat engines fueled by combustion or nuclear fission. Other types of sources could be kinetic energy of flowing water and wind or sunlight. In the Czech Republic the most used resource for electricity generation are coal-fired power plants (47 %), the second highest generation is from nuclear power plants (35 %), the rest electricity is generated from gas-fired power plants, solar power plants, wind power plants, etc. The electricity production ratio can be seen in the Fig. 1.1. The Czech Republic is mostly exporting electricity to the border countries to compensate their deficit. That means that the Czech Republic is self-sufficient.

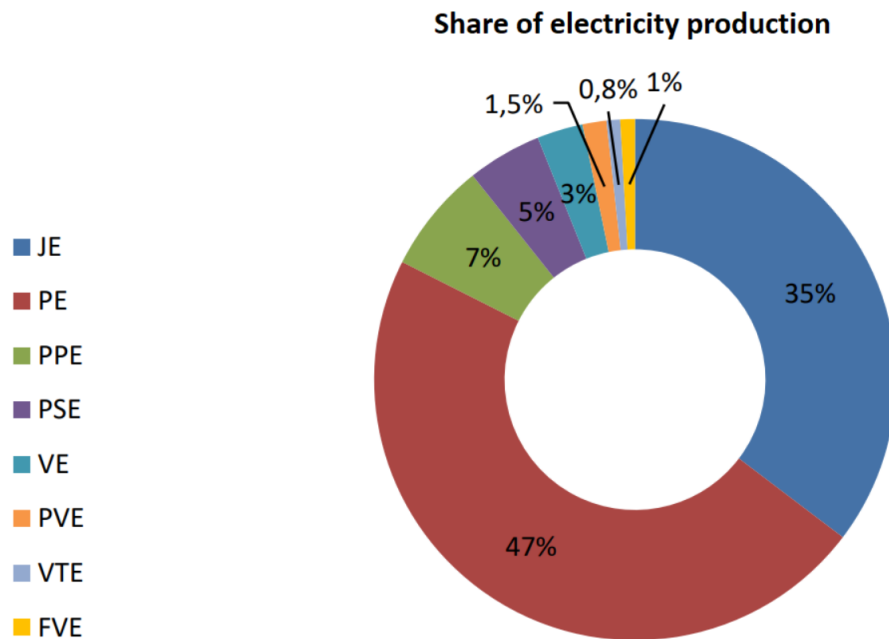


Figure 1.1: Share of electricity production by source (2020)[1]

The transmission of electricity is a bulk movement of electricity from a generating site to a substation. The interconnected lines which facilitate this movement are known as a transmission network. This network is the main target of research in this thesis. The inferior network of the transmission line is distribution line, which conducts electricity between substations and consumers. The operator of the Czech transmission line is ČEPS, a. s., which is state-owned company. The transmission grid in the Czech Republic consists of lines of voltage levels 400 kV, 220 kV and 110 kV. The distribution network voltage level is 110 kV and in the Czech Republic and is operated by companies ČEZ Distribuce, EG.D (till 2020 E.ON Distribuce), and PRE-distribuce. These companies differ in the location of operation, most of the Czech Republic power distribution network is operated by ČEZ Distribuce company.

For the smooth power supply of all consumers it is necessary to ensure all system components of the power system work without failures or voltage or frequency fluctuation, that might cause serious issues. The quality of the electric power supply is based on several parameters, which include for example continuity of service, voltage magnitude variation, transient voltages and currents, and harmonic distortion. The grid frequency in the synchronous grid in the continental Europe has a nominal value of 50 Hz.

A wide variety of events can cause disruption of the power system that might lead up to the blackout, which should be avoided. Among the events that can cause blackout belongs also a solar storm, which consequences will

Chapter 2

Literature review

2.1 GIC

2.1.1 Introduction

Among the potential threats to power system stability and availability, that should be studied, belongs also geomagnetically induced currents. GICs are related to time variations of the geomagnetic field of the Earth. The generation of GICs follows from the Maxwell's equations. The GICs are a manifestation of space weather at the ground level. During space weather events, such as a solar storm, electric currents in the magnetosphere and ionosphere experience large variations, which manifest also in the Earth's magnetic field. These variations induce GICs in conductors operated on the surface of the Earth. Electric transmission grids and buried pipelines are common examples of such conductor systems. GIC can cause issues, for instance, increased corrosion of pipeline steel and damaged high-voltage power transformers. GICs are one of the possible consequences of geomagnetic storms, which may also affect geophysical exploration surveys and oil and gas drilling operations.[2]

This chapter will contain these topics: Space weather, Maxwell's equations, GIC generation, Potential effects on the power grid system components cause by the GICs, Events associated with GICs and GIC studies in the world. The first topic will explain the phenomena of space weather, its causes and effects, it will explain how are solar storms affecting the systems on Earth surface. The topic Maxwell's equations will explain the mathematical equations describing vectors of electric and magnetic field. In next topic, I will briefly explain the GIC generation based on the Maxwell's equations and also its possible consequences. In this chapter, there will be mentioned some of the most important events and its consequences in the past and studies from countries that conducted research on GICs.

stable fast solar wind stream interacts with the surrounding slow solar wind in the low and middle latitude regions of the heliosphere. [6]

The effects of the space weather on the Earth's surface are many. The first observed and explained effect was aurora, that is most often visible in the higher latitudes. The aurorae are a consequence of the collisional excitation of the nitrogen and oxygen atoms by the accelerated charged particles, originating from the Sun, followed by the radiative de-excitation. [7] The effects on the Earth might be negative, for example space weather can influence function and reliability of devices installed on the Earth's surface or in space. In the past, there were observed problems with the communication systems, especially telegraphs, and interference with radio transmissions or navigation systems for aircraft and marine traffic. Another disruptions that might be caused by solar activity and might affect our everyday lives are GICs, that are induced on the power grids or buried oil and gas pipelines as these are common examples of conductor systems. Another conductor systems, that might be affected by the GICs are non-fiber optic undersea communication cables, non-fiber optic telephone and telegraph networks, and railway signalling networks.

■ 2.1.3 Maxwell's equations

The equations provide a mathematical model for electric, optical, and radio technologies, such as power generation, electric motors, wireless communication, lenses, radar, and others. There are four double (differential and integral form) Maxwell's equations, that are partial differential equations that form the foundation of classical electromagnetism, classical optics, and electric circuits. The Maxwell's equations describe how vector electric (\mathbf{E}) and magnetic (\mathbf{B}) fields are generated by charges, currents, and changes of the field. [8]

First Maxwell's equation is the Ampere's law. The Ampere's law allows us to calculate magnetic fields from the relation between the electric currents that generate this magnetic fields.

$$\oint_C \mathbf{B} \cdot d\mathbf{l} = \mu_0 I + \frac{d\Psi}{dt}, \quad (2.1)$$

where the integral is taken around a closed curve C . I is conductive current and Ψ is a electric-field flux passing through a surface enclosed by curve C . The parameter μ_0 represents the constant of magnetic permeability.

Second Maxwell's equation is the Faraday's law of induction. This law is predicting how a magnetic field will interact with an electric circuit to produce an electromotive force known as a electromagnetic induction. This equation describes that spatially or time varying electric field always accompanies time varying magnetic field or vice versa.

$$\oint_C \mathbf{E} \cdot d\mathbf{l} = -\frac{d\Phi}{dt}, \quad (2.2)$$

where Φ is a magnetic inductive flux enclosed by curve C . Again, the integral is taken around a closed curve C .

Third Maxwell's equation is the Gauss's law that describes the relationship between a static electric field and the electric charges that cause it.

$$\oint_C \mathbf{D} \cdot d\mathbf{S} = Q, \quad (2.3)$$

where \mathbf{D} is a vector of electric induction in coulomb per square meter in a closed surface S enclosing any volume V , Q is the total charge enclosed within V . The quantity \mathbf{D} is directly related to the electric field \mathbf{E} , where ϵ_0 stands for vacuum permittivity.

$$\mathbf{D} = \epsilon_0 \mathbf{E} \quad (2.4)$$

Fourth Maxwell's equation is the Gauss's law for magnetism, it states, that magnetic induced flux of any closed oriented surface S is equal to zero. It is equal to the statement that magnetic monopoles do not exist.

$$\oint_C \mathbf{B} \cdot d\mathbf{S} = 0 \quad (2.5)$$

The GIC generation follows the second Maxwell's law, the Faraday's law of induction by the change of magnetic field of Earth and will be further described in following chapters.

■ 2.1.4 GIC generation

$$\nabla \times \mathbf{E} = -\frac{\partial \mathbf{B}}{\partial t} \quad (2.6)$$

The differential form of the Faraday's law of induction, where \mathbf{E} is a vector of the intensity of electric field and \mathbf{B} is a vector of magnetic induction says, that the electric field on the Earth surface depends on the time variation of the Earth magnetic field. In our case, both quantities are measured near the ground.

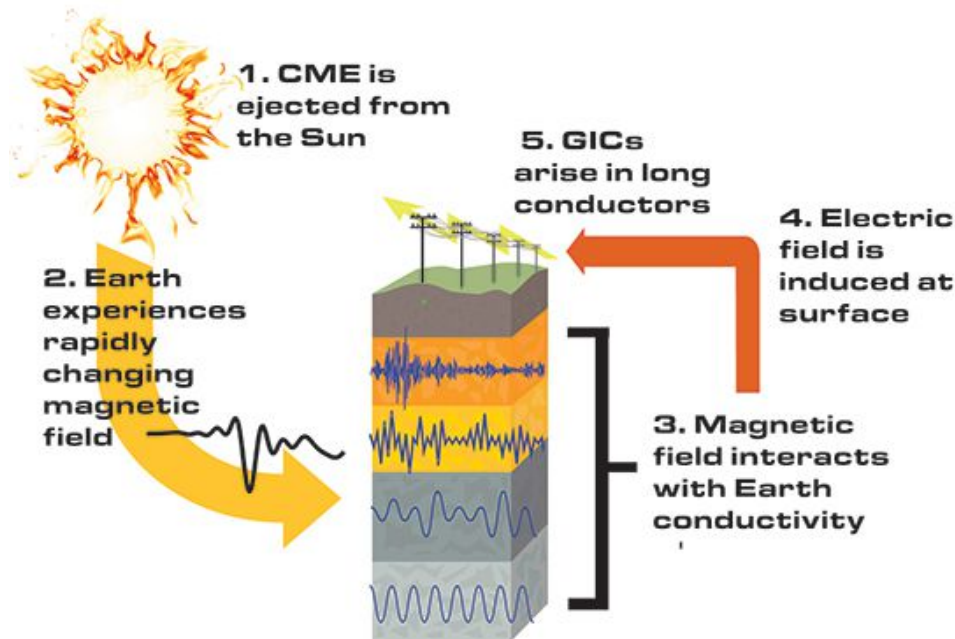


Figure 2.1: The chain of events from a coronal mass ejection (CME) on the Sun to geomagnetically induced currents (GICs) in transmission lines [9]

During electromagnetic storms that affects the Earth, a change of magnetic field occurs near the Earth. The time variations of this magnetic field cause secondary magnetic field on the Earth. A very rapid and significant change in the intensity of the Earth's magnetic field leads to change of the magnetic flux on a certain surface, and this causes creation of a geoelectric field; the geoelectric potential of this field is in the order of units V/m. This geoelectric potential has a character of voltage source between the conductor systems. Through the phase windings of the transformers, these currents flow into electrical systems. The process of GIC generation is shown in the Fig 2.1.

The amplitudes of the GICs depend on many variables. For the calculation it is important for us to know the electric field time variation during the studied time period, the location at the Earth's surface and parameters of the affected conductive line. As the GICs have a cumulative character, it is also important for us to know the parameters of the grounded power transformers in the substations and also the individual GIC contributions of the power grids that lead into the investigated substation. In our case we consider the substations as grounded nodes connected by the transmission lines.

The variation frequency of GICs is governed by the time variation of the electric field. The period of change of the GICs is in the order of seconds up to hours, that means that the GICs are considered to be quasi direct currents. For our purpose we will consider the GICs to be direct current (DC).

2.1.5 Potential effects on the power grid system components caused by the GICs

If the transformer is subjected to a DC, then it results into an unidirectional DC flux in the transformer core. In the figure 2.2 it is shown a magnetisation curve of a transformer, the ratio of flux density to field strength (B/H). The blue curve represents the curve for a sinusoidal current flux (AC current), for red curve (AC+DC current) there is a visible change of the saturation point value, which in this case shows a state that we call magnetic saturation or saturation of the core. The magnitude of this flux depends on the magnitude of the DC, number of turns in the windings carrying the DC current and reluctance of the path of this DC flux. The issue of the DC in the transformer core is the fact, that the DC flux is added to the AC in one half of the period and in the other half it is subtracted from the AC. If the DC flux is large enough, then it causes a core peak flux densities in the magnetic core of the transformer and it leads to a pre-saturation.

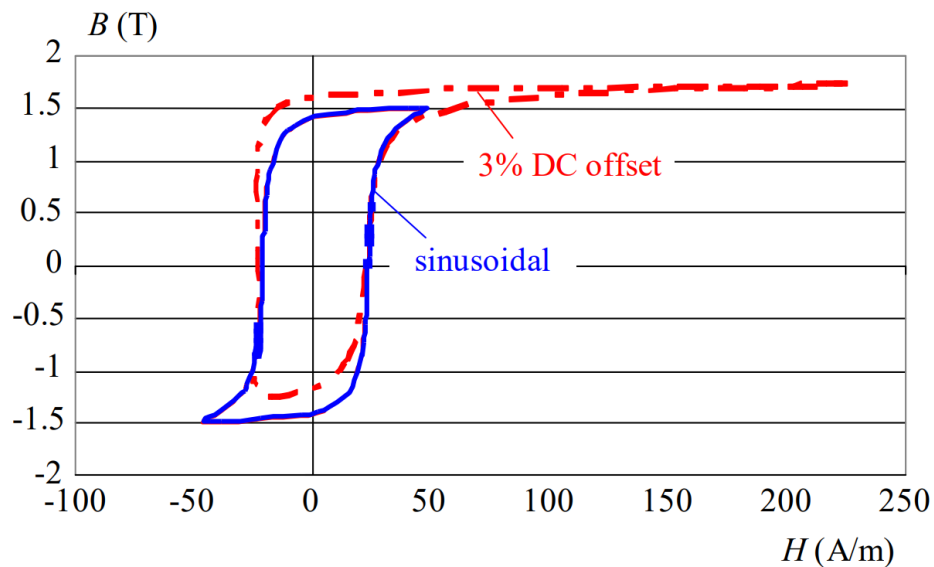


Figure 2.2: Effect of 3% DC offset in the input voltage on the B-H loop [10]

In order to accurately determine the capability of a transformer to GIC, we need to consider the nature of the signature of the GIC current as well as magnitudes and time duration involved with a GIC event.

2.1.6 Events associated with GICs

In this chapter, will be briefly summarised main events and their consequences of space weather that are associated with extreme geoelectric field and geomagnetically induced currents all over the world. Most of the events described occurred in the area of higher latitudes or where the ground conductivity was

higher, hence GICs were expected to gain higher values. Also in countries sparsely populated, where the distances between two grounded substations are bigger, the expected values of GICs are larger, the GIC amplitude is proportional to the length of the line.

The largest horizontal geoelectric field magnitude reported in the literature was 45 – 55 V/km in northern Norway in March 1940. These values were estimated from the effect that the substation components experienced. The highest directly measured values of geoelectric field magnitude were about 10 V/km. The largest GIC measured in the Finnish 400-kV power system since the beginning of the recordings in 1977 was as high as 201 A in the transformer neutral lead at the Rauma station in southwestern Finland on 24 March 1991.[11]

■ Carrington event

The Carrington event that occurred on 1–2 September 1859 is the strongest storm ever recorded, that had affected mainly telegraph equipment. On 1 September two amateur astronomers Richard Carrington and Richard Hodgson independently observed and recorded the first solar flare in history. A day after the observation of solar flare, in the Kew Observatory very large geomagnetic field variation were recorded and Carrington suspected a solar-terrestrial connection. World-wide reports on the effects of the geomagnetic storm of 1859 were compiled and published by American mathematician Elias Loomis, which supported the observations of Carrington and Stewart.[12]

There were several effects of that geomagnetic storm on the Earth and some of them were visible by the human eye. For example, the aurorae, that are usually visible only in the arctic areas, were visible even at lower latitudes – in the Caribbean, Mexico, Hawaii, Japan, China, etc... The aurorae were so strong, that people were able to read newspapers at night by the aurora's light and some people woke at night because they thought that it was a daylight. Another more serious effect were failures of some telegraph systems all around the world, that in some cases lead up to the injury of the telegraph operators by giving an electric shock caused by the geomagnetic induced currents on the telegraph lines. [12]

If solar storm of this magnitude would occur today, it might lead up to the widespread electrical disruptions, blackouts and damage due to extended outages of the electrical grid. The reason is that nowadays all transmission lines in continents are connected and if the outage of several transformers occurs, it might lead up to the disruption and finally to a blackout due to grid frequency change or voltage level variation, etc. [12]

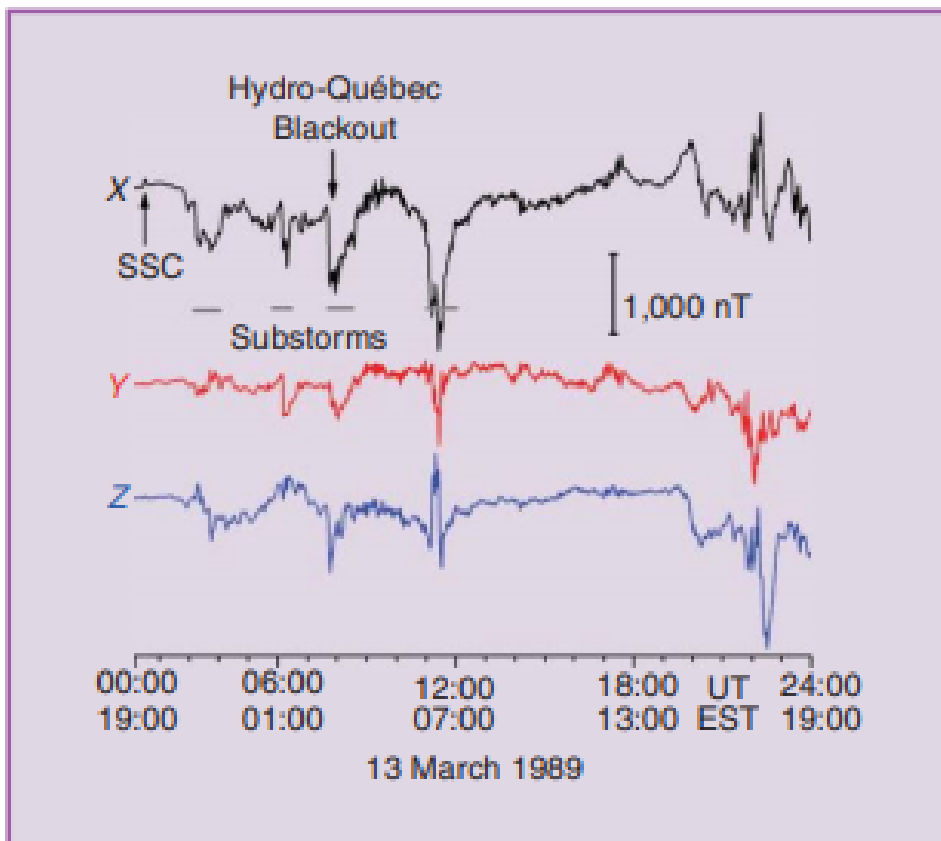


Figure 2.3: The sequence of magnetic disturbances experienced in Quebec on 12-14 March 1989 [16]

The moment when the cloud of plasma from the Sun arrived to the magnetic field of the Earth is shown in the figure 2.3 as a sudden storm commencement (SSC), here we can see a sharp jump in the magnetic field. After that point we can see several other jumps that are known as substorms. The substorms are caused by the solar wind that compresses Earth's magnetosphere on the side facing Sun (day side) and draws the magnetic field lines out into a comet-like tail on the night side. Some of the solar wind energy is dissipated as it flows around our planet, but some is stored in the magnetic tail and releases substorms. During the substorms the charged particles are ejected from the magnetic tail toward the Earth and followed the magnetic field lines into the high-latitude regions. [16]

What else we can see in the figure 2.3 is the point when the Hydro-Quebec blackout occurred. The substorm that caused the blackout was the third one in a row. The first substorm visible in that figure did not cause troubles, but the second substorm caused GIC disturbances in the Hydro-Quebec power system that lead to the voltage fluctuations – fortunately, the operators had time to do react. Unfortunately, the third substorm caused the saturation of many power transformers in the Hydro-Quebec power system and they

draw more reactive power – they were a source of higher harmonics. The other problem was, that the static var compensators that might have been sources of reactive power to compensate the reactive power were tripped out of service due to the high harmonic currents. After the loss of the dynamic voltage support, the system was unstable. The voltage drop lead to the line tripping and the system was disconnected that lead again to the voltage drops in other generating stations. The other effect was the frequency drop and a loss of approximately 9 500 MW of generation from the La Grande complex. This all caused the collapse of the system. The single failures of the system are shown in the figure 2.4. [16]

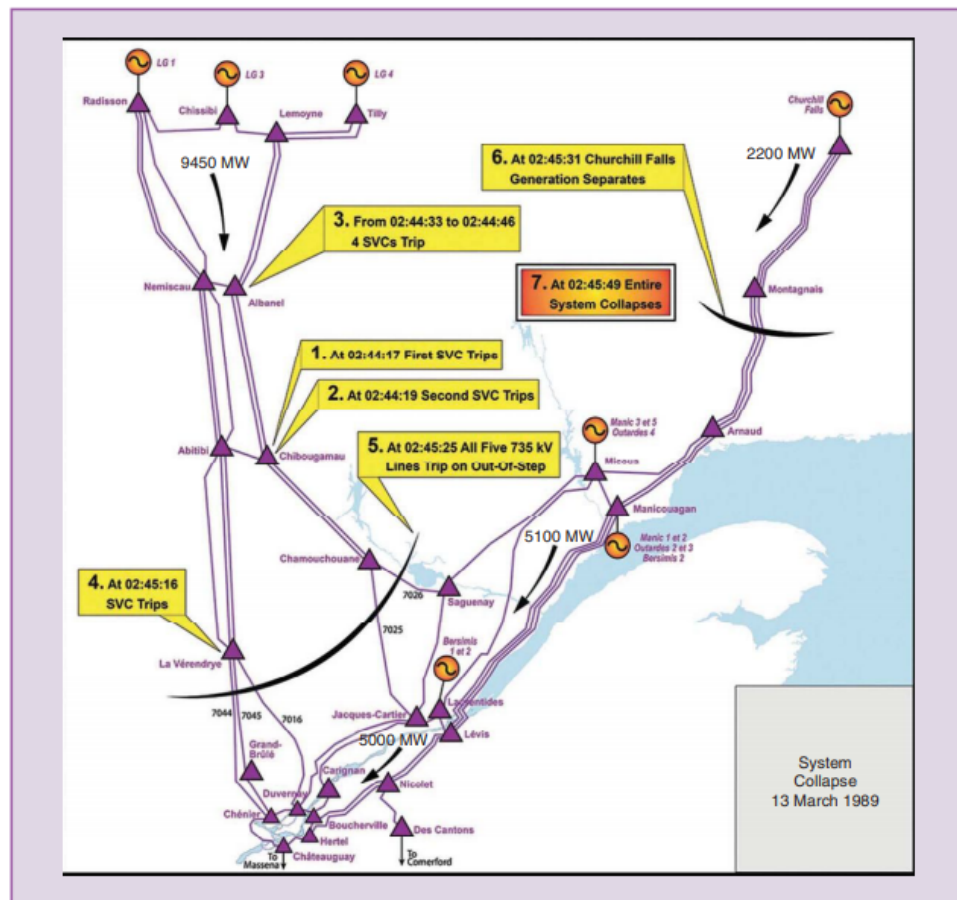


Figure 2.4: The location of principal events leading to the blackout [16]

The real problem occurred, when the induced currents found weakness – the 735-kV power lines. The lines, compared to the Czech transmission grid, are longer and the subsoil is mostly a large rock shield. The currents have found the less resistant path, that caused tripped circuit breakers within two minutes and caused a blackout. The blackout affected all area of province of Quebec, where the power grid had lost power for about nine hours. [17]

This blackout lasted about nine hours and also led to the power losses in the power grids of the New York City, where the losses were about 150 MW, in the New England, the power losses were even higher, about 1410 MW. The problems caused could be even greater if other electric energy sources would not even partially cover these losses. It might have led up to the electric power grid breakdown and cause another blackouts, that might have been more serious.

■ Halloween storms

At the end of October 2003 the complex of solar storms occurred and affected the Earth. The geomagnetic storm began on the 28 October with coronal mass ejection and lasted for more than 27 hours. Fortunately, the direction of the cloud of electrified gas ejected was not straight towards the Earth but at an angle of 20 degrees, so the effects were not so serious as it might be, but nonetheless, the effects were serious.[18]

For example, several satellites in the space were highly affected. More than half of the deep space and near-Earth space science missions experienced effects of the storm. The Solar and Heliospheric Observatory (SOHO) satellite, a collaboration between NASA and the European Space Agency (ESA), failed temporarily. NASA's Advanced Composition Explorer (ACE) satellite experienced damage, and instruments aboard many spacecraft had to be shut down temporarily.[18]

Same as for the previous events, the aurora was visible from places that are not usual. For example Florida, Texas, etc. Due to the problems with the communication canals, there were many secondary effects of this storm. For example the US army had to cancel maritime missions, airborne magnetic and geophysical surveys were delayed or cancelled, and the GPS location was not so accurate.[19]

The most significant effect of the Halloween storm of 2003 was the blackout, that affected the Swedish power grid – specially the city of Malmö. The GICs, that were generated and flowed in the transmission line reached values of hundreds of Amperes. The reason why the blackout occurred was the excess heating in the power transformer and tripping of a 130-kV line by relays, that had high sensitivity to the third harmonics that was the effect of the GICs. The blackout lasted for about one hour at the evening of 30 October and affected about 50 000 customers in Sweden.[20]

In the Sweden power grid, there are installed measuring systems of GICs, the continuous measurements have a one minute resolution. For the Halloween storms, measured data near Simpevarp-1 substation are limited to 29 October and the morning of 30 October. Unfortunately, there are no other data because of the problem with monitoring system that failed the measuring

system to record the data, so the GICs for this event that caused blackout had to be calculated. The value of calculated GICs at Simpevarp-1 reaches a peak value of about 330 A a few minutes before the time of the Malmö blackout.[20]

■ 2.1.7 GICs studies in the world

Because of the very high importance of problems caused by GICs in the high-geomagnetic-latitude areas, there were already made several studies in different countries all over the world. Mostly, these studies were made in the countries where more serious issues may be expected. In the literature, two factors are recognised as important. First, the locations on the Earth (the areas closer to geomagnetic poles are expected to be more sensitive to the changes of the geomagnetic field) and second, the line length (the amplitudes of the GICs are proportional to the line length). In next paragraphs will be mentioned the main studies in various areas of the world.

■ Finland and Great Britain

In the study [21] the events were investigated, which were associated with the GICs on the 6-7 April 2000 in the Great Britain and Finland. During this event large GICs were measured in the technological system in both countries.

The currents were measured in the neutral line connecting the three phases of the power transformer to the ground. The source of those GICs were mostly substoms, that were discussed in the previous chapter. In this case, during this event, the peaks lasted just for several minutes, typically not longer than for 15 minutes. According to the study we know that the GICs forecast depends on the substoms predictability. This might give the operators of the TSOs enough time to react to the possible coming danger. [21]

■ Austria

As Austria is one of the neighbouring countries to the Czech Republic and it recently made its own study for GIC modelling, we have a very good opportunity to compare modelled values from this country with the values modelled for the Czech Republic. The ground conductivity and the location on the Earth of these two countries are similar and there should not be significant difference between modelled values.

The study was conducted in Austria after 2014 and consists of two parts. First part of this study was the modelling of geomagnetically induced currents using Lehtinen-Pirjola method, that will be further explained, for the Austrian Power Grid and the second part was comparison of the GICs modelled and GICs measured in the substations. The reason to start the research was

that during commission of new transformer in 2014, unexpected noise and saturation of the transformer due to DC was observed, so Austrian Power Grid operator decided to conduct this study.[22]

In this research, one of the main goals was to model values and GIC effects during extreme geomagnetic storms that might occur, based on the power grid parameters and ground conductivity, that differs in the different areas in Austria mainly. A particular interest was given to the region of the Alps, where the bedrock has a much larger resistivity than in the rest of the country. The bedrock resistivity influences the amplitude of the horizontal components E_x and E_y of the geoelectric field as follows from the integrations of the Faraday's law under a plane-wave approximation [23]:

$$E_y(t) = -\frac{1}{\sqrt{\pi\mu_0\sigma}} \int_0^\infty \frac{g(t-u)}{\sqrt{u}} du, \quad g(t) = \frac{dB_x}{dt}, \quad (2.7)$$

and correspondingly for E_x . In the equation above σ represents the bedrocks conductivity. The larger bedrock resistivity (lower conductivity) is connected with the larger amplitudes of the geoelectric field under the condition of the same variations of the geomagnetic field. The GICs are then proportional to the magnitude of the geoelectric field, hence the regions with a larger bedrock resistivity are considered as regions with a higher risk from GIC effects.

As mentioned before, the Czech Republic and Austria are both located in the mid-latitude area, where the GIC values are not expected to be significant enough to have a big impact on the grid components to cause serious damage. However, mainly due to the Alps, the assumption is, that amplitudes of GIC in Austria might be compared to the zone of Denmark or Scotland. [22]

The measurement system installed in Austrian power grid measures DC currents and has a cut-off level of ± 2.4 A, that unfortunately limits more exact analysis, because this value was exceeded several times for several minutes during the measurements.[22]

By modelling the GIC they received current values for the period of Halloween storms in 2003, the maximum values of GIC modelled were 8.98 A, 1.91 A and 6.42 A for the three chosen nodes. Assuming, that the model tends to underestimate the values by 49%, the maximum value during the Halloween storm in Austrian power grid was 13.38 A. As mentioned before, the study consisted of validation of model with modelled and measured data and evaluation of sensitivity of the varying network topologies.[24]

■ Italy

The study from Italy was published in 2018 and followed up GICs in Italy during the St. Patrick's day storm in 2015. Even though Italy is located in lower-latitude area (compared to the most affected countries like Sweden,

Denmark, USA, Canada,...), due to the Alps on the north of the country, where is a lower ground conductivity, the GICs are necessary to investigate. Because of the low conductivity of the ground, the currents are more tend to flow to the transmission grid, as they flow along the lower resistance path that is in in this case power grid. [25]

According to the conclusion of this research, the risk of GIC for Italy is considered to be moderate. The north of Italy is more exposed to possible damage of power grid components by GIC events then the rest of Italy. Modelling the GICs with the value of geoelectric field of 1 V/km (this value is associated with extreme geomagnetical storm), the amplitudes for Northern Italy were calculated as 97 A, which is considered to be very high value, that might cause significant damages on the power grid components. But also for regions on the south, the values were not negligible. [25]

■ Spain

For the research of GICs in Spain, the model used for GIC calculation for this study is the same as the one used for this thesis. The model was also validated with measurements from measurement system installed in one of the transformers. The model of Spanish power grid for GIC calculating consisted of 17 nodes (substations) and 23 transmission lines of the 400-kV voltage level grid. [26]

The geomagnetic storm modelled and measured in their study occurred on 24-25th October 2011. The geomagnetic records were achieved from the Ebro geomagnetic observatory on the South of the country. In the graph that is shown in figure 2.5 we can see the time evolution of GIC currents measured and modelled so we can compare both values. According this study, the Pirjola model for calculating GICs provides a satisfactory GIC model which is comparable to the measured values. [26]

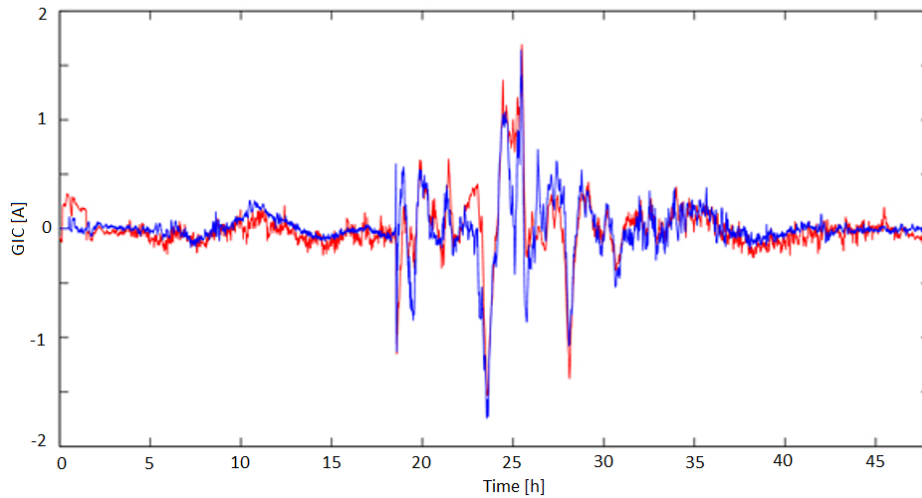


Figure 2.5: Measured (red) and calculated (blue) GIC at the TR2 transformer of Vandellòs for the event of 24–25 October 2011. [26]

■ Czech Republic

As GICs are not affecting only transmission lines, but also buried pipelines, another type of conductor system, which were the subject of another research in the past. In the Czech Republic, there are two oil pipelines, IKL and Družba shown in the figure 2.6. The Družba pipeline was built by the Soviet Union in 1960's and it is the longest oil pipeline in the world (4000 km), it carries oil from eastern part of Russia to Europe. The IKL pipeline was built in 1990's and carries oil from Ingolstadt to the Czech Republic. As the Družba and the IKL pipeline were built in distinct epochs, they differs in several parameters. [27]

This research, which was examining the GIC induced in the gas pipelines in the Czech Republic, started after the 2003 Halloween storm, when the pipeline operator observed irregular currents. The main reason, why do we have to examine the currents in the pipeline system is, that the pipeline corrosion is associated with the pipe-to-soil voltage and is damaging the pipeline. The pipelines are protected by insulating coating and with the cathodic protection, which keeps the pipeline at the exact potential (depending on the pipeline coating - for IKL it is -1.2 V and for Družba -2 V). [27]

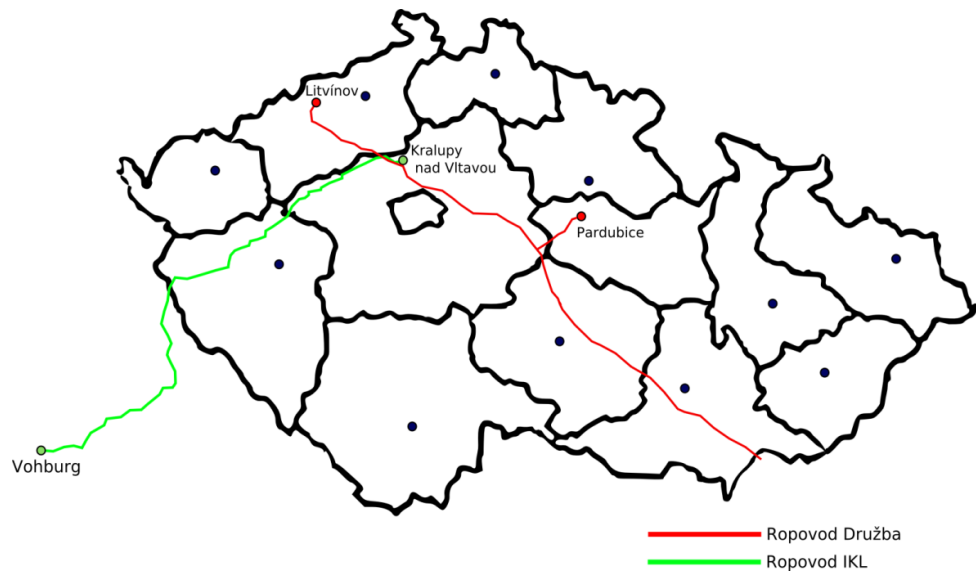


Figure 2.6: Oil pipelines in Czech Republic [28]

Pipe-to-soil (P/S) voltage is measured by the pipeline operator at about 80 stations in Czech Republic. For this study, data from 3 of them were used. The measured P/S voltage data were directly compared with the calculated geoelectric field, which itself was calculated by the simplest plane wave model. The two time evolutions were compared and are shown in a graph 2.7 and as can be seen, that the data correspond to each other. The study [27] showed that most of the P/S variations during Halloween storms may be attributed to the spaceweather effects.

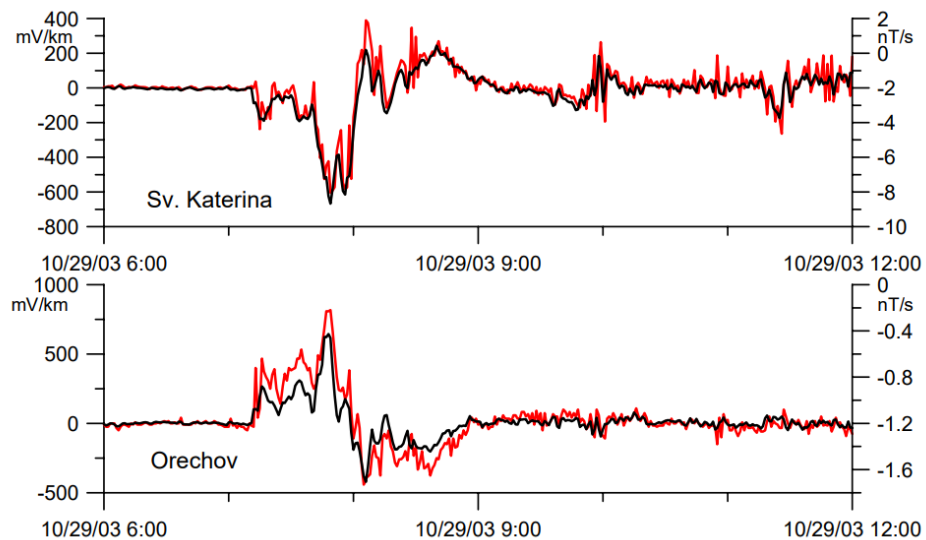


Figure 2.7: Fit between the measured P/S voltage (red) and the computed geoelectric field (black) for the most disturbed period of 29 October 2003 [27]

Another researches were conducted in the Czech Republic. The goal was to investigate a statistical correlation between the occurrence of disturbances on the electric power transmission network in the Czech Republic and the geomagnetic activity described by the K index, which is typical for characterizing the level of geomagnetic activity in similar applications. The maintenance logs were provided by the power grid operators (both transmission and distribution lines). The maintenance logs were divided into 12 separate sets when the events were divided according the affected device or voltage level. The events, that could not be associated with GICs were excluded from those sets. The authors found that in case of the data sets recording the disturbances on power lines at the high and very high voltage levels and disturbances on electrical substations, there was a statistically significant increase of anomaly rates in the periods of tens of days around maxima of geomagnetic activity compared to the adjacent minima of activity. There were hints that the disturbances were more pronounced shortly after the maxima than shortly before the maxima of activity. The results provided indirect evidence that the geomagnetically induced currents may affect the occurrence rate of anomalies registered on power-grid equipment even in the mid-latitude country in the middle of Europe. [29]

The study was followed by another study [30], where the authors investigated the near-immediate effects of the exposure of the Czech power grid to spaceweather events. A superposed epoch analysis was used to identify possible increases of anomaly rates during and after geomagnetically disturbed days. It was shown that in the case of abundant series of anomalies on power lines, the anomaly rate increased significantly immediately (within 1 day) after the onset of geomagnetic storms. In the case of transformers, the increase of the anomaly rate was generally delayed by 2–3 days. The authors also found that transformers and some electric substations seemed to be sensitive to a prolonged exposure to substorms, with a delayed increase of anomalies. Overall, in the 5-day period following the commencement of geomagnetic activity there was an approximately 5–10% increase in the recorded anomalies in the Czech power grid and thus this fraction of anomalies is probably related to an exposure to GICs.

Chapter 3

Czech transmission line

As mentioned in previous chapter, the Czech transmission line is operated by the company ČEPS, a. s. This company is owned by the state and maintains, restores and develops 41 substations with 71 transformers around all the Czech Republic. The total length of Czech transmission line is 5502 kilometers from which the lines with voltage level of 400 kV are 3508 km long, with voltage level of 220 kV are 1910 km long and the 110 kV transmission lines are 84 km long. The transmission system schema is shown in the Fig 3.1

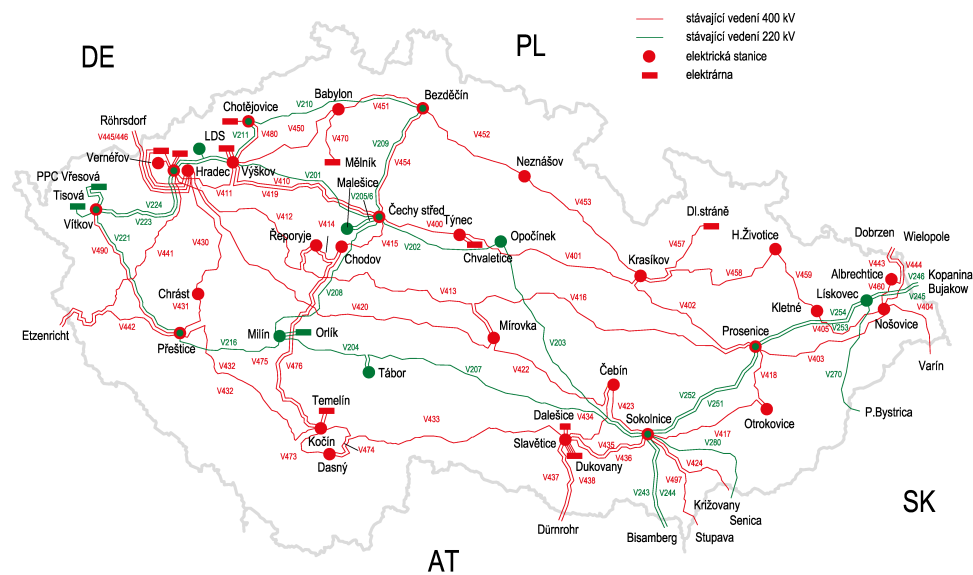


Figure 3.1: Schema of the Czech transmission grid[31]

For our purpose, the focus will be on the transmission line of voltage of 400 kV (in Fig 3.1 with red colour), which leads only to the substations inside of the Czech republic. This criteria meets 57 transmission lines and 37 substations.

3.1 Parameters of the Czech transmission grid

There are many parameters of the power grid which are monitored and are important for designing of transmission lines and their smooth operation. For example it is important to dimension the line according to consumption of energy in cities or according the production in power plants. On the map in figure 3.1, we can see that big substations are situated near Prague, Brno or near the two Czech nuclear power plants – Dukovany and Temelín.

For our calculations the main parameters are:

1. Line length

The most important parameter for GIC calculation is the distance between two grounded substations. A bigger distance leads to higher amplitudes of GIC generated on the transmission line. The longest transmission line in Czech republic was line 413 from substation Prosenice to substation Řeporyje, which was in year 2019 divided into two lines – 413 and 416. Now, the longest transmission line is line 420 which leads from substation Hradec to substation Mírovka. This line is almost 210 km long.

2. Line orientation

Another very important parameter is the orientation of the transmission line, which states the longitude and latitude of the transmission line. This parameter is important because of the geoelectric field which differs in the direction from north to south and east to west. Higher amplitudes of the GIC are expected in the power lines which are oriented from north to the south.

3. Electric parameters

Longitudinal impedance Z

$$Z = R + jX \quad [\Omega/\text{km}], \quad (3.1)$$

where R is resistance and X is inductive reactance. The resistance is the real part of the impedance and the reactance is the imaginary part. The value of imaginary part of the impedance depends on the frequency and is usually shown by a coil.

$$X = \omega L = 2\pi fL \quad [\Omega/\text{km}], \quad (3.2)$$

where f is frequency.

For our purpose this parameter will be characterized by the length of the line and the line resistance. As the value is directly proportional to the length and the resistance, the longer is the line or the bigger DC

resistance the line has, the bigger its impedance is. And according to the Ohm's law, the bigger the impedance is, the lower are the values of currents induced on the transmission line. Unfortunately, with the value of resistance also the power losses grow, which means financial losses. It is very important for the power grid designers to consider that fact in their calculation to find the best value of the line resistivity which is given by the selected conductor.

Transverse admittance \mathbf{Y}

$$Y = G + jB \quad [S/km], \quad (3.3)$$

where G is a conductance and B is a susceptance. As in the equation for impedance, the conductance is the real part of admittance and the susceptance is an imaginary part of admittance. In the conductor system it is shown by a capacitor.

$$B = \omega C = 2\pi f C \quad [S/km], \quad (3.4)$$

where f is frequency.

For our purpose this parameter will be characterized by the substation grounding resistance described below.

Whereas the GICs are assumed to be DC, the only part of above equations we need to include to our calculation is the real part of the equations. The imaginary part of the equation is dependent on the frequency and for our purpose we assume it is equal to zero. This approach is justified because the modelled GICs vary in time very slowly, with frequencies much lower than the usual power frequency. GICs may be considered DC in the first approximation.

Whereas the transmission line can be simplified into the conductor system, according to the Ohm's law, every conductor system is described with the resistance, voltage and current. This simplified law will be used in our case, so for calculation of the current, the resistance is needed to know. The highest value of resistance for our selected lines has the line number 420 and is 5.91 Ohm. The Ohm's law is simply given by

$$I = U/R . \quad (3.5)$$

4. Substation grounding resistance

This parameter is very hard to determine, because it is only measured when the substation is built or reconstructed and its value can also change during the substation operation. This parameter depends on the

conductivity of the ground – soil composition in a given place, mineral content, characteristics Earth's envelope to a depth of approximately 100 kilometers, but also humidity, temperature and climatic conditions at the time of measurement.

The values of the grounding resistance are in tens or hundreds of miliohms.

Thanks to ČEPS, a. s., that has provided data for this thesis, data of the lengths, resistance and coordinates on the Earth surface are provided for each line. Unfortunately, the values for substation grounding resistance are available only for several substations.

Chapter 4

Lehtinen-Pirjola method of GIC calculation

In the ideal case, the GICs could be measured with sensors intended for this purpose. Unfortunately, these sensors are rare and expensive, so they were installed only at a few points in the power grids with higher risks to GICs-related damages. The sensors are being installed on the neutral conductor of large substation transformers and sense the DC current without making electrical contact. In the Czech Republic the one and only sensor was installed in the substation Mírovka [32]. This measurement system consists of two sensors both are current sensors. First sensor is a commercially available current sensor with Hall probe, the other one is fluxgate based current sensor, that was developed by Ing. Pavel Mlejnek, Ph.D., from Czech Technical University in Prague. The current measured by the measurement system consists of two components – AC and DC. The AC is caused by the transmission system disruptions The DC component might be caused by the GICs or by the return or stray currents. [33]

Several studies from several countries showed that the GICs may successfully be modelled. The modelled values were satisfactorily comparable to the direct measurements. The advantage of the GIC modelling is that it is very cheap compared to the development, installation and maintenance of the GIC sensor, and that the modelling may be performed for any situation for which the measurements of the geomagnetic field is available. Thanks to the international network of geomagnetic measuring stations Intermagnet, the necessary measurements are available for a dense set of measuring stations, with a very long time coverage and a very large duty cycle approaching the value of 100%. Recent studies showed convincingly that the values obtained from the sensors do not differ much from the values obtained from the equations below, so we can consider these equations to be sufficient for the purpose of this thesis.

The method for calculating the GICs generally used and tested in literature bears the name of its authors, Lehtinen and Pirjola. The method stems from the direct application of the Kirchoff's laws, when the power-distribution network was virtually replaced by the electric circuits.

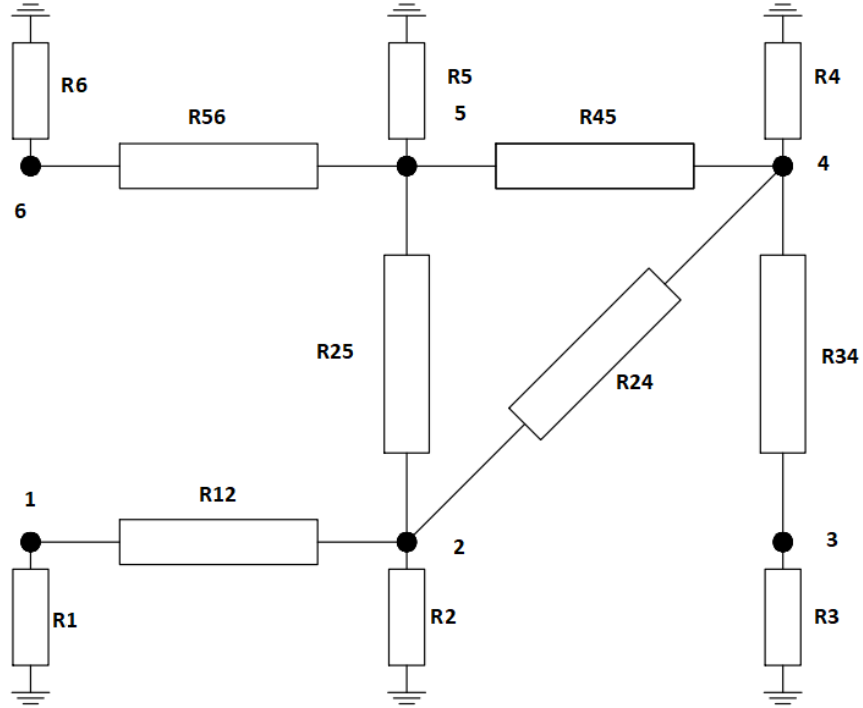


Figure 4.1: Scheme of the electrical circuit representing a fictional power grid with six nodes. This scheme demonstrates one of the inputs to the Pirjola-Lehtinen method of GIC calculation

The network consists of N grounded nodes (with known grounding resistances) that are connected by the power lines with a known resistivity. For example, the fictional power grid scheme is shown in Fig 4.1, where the nodes are represented with a dot with grounding resistance R_i value and power lines with its resistance with a R_{im} value. The lines are subjects of the induction by the external electric field. The method leads to the following set of equations: [34]

$$\mathbf{I}_e = (\mathbf{1} + \mathbf{Y}_n \cdot \mathbf{Z}_e)^{-1} \cdot \mathbf{J}_e, \quad (4.1)$$

where \mathbf{Y}_n admittance matrix, \mathbf{Z}_e impedance matrix of the whole transmission system and \mathbf{J}_e is a matrix of current flowing through the line under the assumption of the so-called perfect grounding. The matrix $\mathbf{1}$ is an identity matrix $N \times N$. The resulting currents \mathbf{I}_e are the sought GICs flowing through the grounding line of the respective node. The convention is such that the positive \mathbf{I}_e indicates the current flowing from the network to the Earth, negative \mathbf{I}_e occurs when the current flows from bedrock to the network.

The ideal-earthing currents \mathbf{J}_e are given by

$$\mathbf{J}_{e,m} = \sum_{i=1, i \neq m}^N \frac{V_{im}}{R_{n,im}}, \quad (4.2)$$

where V_{im} is geomagnetic voltage calculated from equation (4.3) and N is the number of earthed nodes which represent transformer substations, of entered power network system. $R_{n,im}$ is resistance of wires between the nodes i and m .

The voltages are computed from the known geoelectric field \mathbf{E} by

$$V_{im} = \int_i^m \mathbf{E} \cdot d\mathbf{s}, \quad (4.3)$$

where the voltage is integrated along the curve representing the respective line between nodes i and m . V_{im} is anti-symmetric to the swapping of i and m due to the opposite orientation of integration paths.

The admittance matrix \mathbf{Y} is defined by relation

$$Y_{n,im} = -\frac{1}{R_{n,im}} \text{ for } i \neq m \text{ and } Y_{n,im} = \sum_{k=1, k \neq i}^N \frac{1}{R_{n,ik}} \text{ for } i = m, \quad (4.4)$$

where $R_{n,im}$ is resistance between two grounded nodes represented by the multiple of the value of resistivity of the transmission line and the length of this transmission line. This definition has an advantage for the nodes that are not directly connected by the power line. The resistivity of this ‘‘line’’ is infinite and hence it’s contribution to the admittance matrix naturally vanishes.

The impedance matrix \mathbf{Z} is defined by relation

$$Z_{e,im} = R_i \text{ for } i = m \text{ and } Z_{e,im} = 0 \text{ for } i \neq m, \quad (4.5)$$

where R_i is the grounding resistance of the appropriate node. In the case when the nodes are spatially separated, the impedance matrix is diagonal.

Chapter 5

Data structure

To fulfill the goals of this thesis I wrote a computer program for the calculation of the GICs. The program was written in the Python programming language and utilises advanced data structures provided by the data-processing packages of this programming language. The code reads in the tables describing the topology of the power grid, reads in the externally provided horizontal components of the geoelectric field and following the equations of the Lehtinen-Pirjola method it computes the modelled GICs in each node of the grid.

The structure that will be needed for calculation of GIC will be specified for each item.

5.1 Coordinates of the transmission line

The coordinates data were provided by the company ČEPS in the Excel files for each transmission line, where coordinates of each tension tower were given. The tension towers are enough for our purpose, as only the calculation of the orientation of the transmission line on the Earth surface is needed. In all of the files were provided coordinates in the S-JTSK system, in some of them where GPS coordinates, so I decided to work with the S-JTSK coordinates because that were provided for all of the transmission lines and there was no need to transfer coordinates to different system.

This system of coordinates is used on the territory of the Czech and Slovak Republic. It is a rectangular system, that was determined in the 1922 by the Czech surveyor Josef Křovák. Both of the coordinates of this system on the territory of Czech and Slovak Republic are positive. The X axis leads from the north to the south and the Y axis leads from the east to west, as shown on the figure 5.1. The zero point for this system of coordinates is located near Saint Petersburg in Russia and both axes display the distance from the zero point to displayed point in meters. Thanks to the size of the Czech Republic, the S-JTSK system is very close to the horizontal components of the Cartesian system, in which the amplitudes of the geoelectric field are given.

The deviations of the Cartesian and S-JTSK systems in the Czech Republic are negligible for the purpose of this thesis.

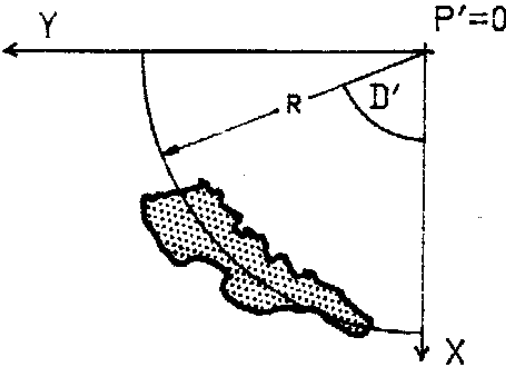


Figure 5.1: S-JTSK coordinates axes [35]

The data of all coordinates were imported and each transmission line plotted into the figure that copies the transmission system map presented in chapter 3.

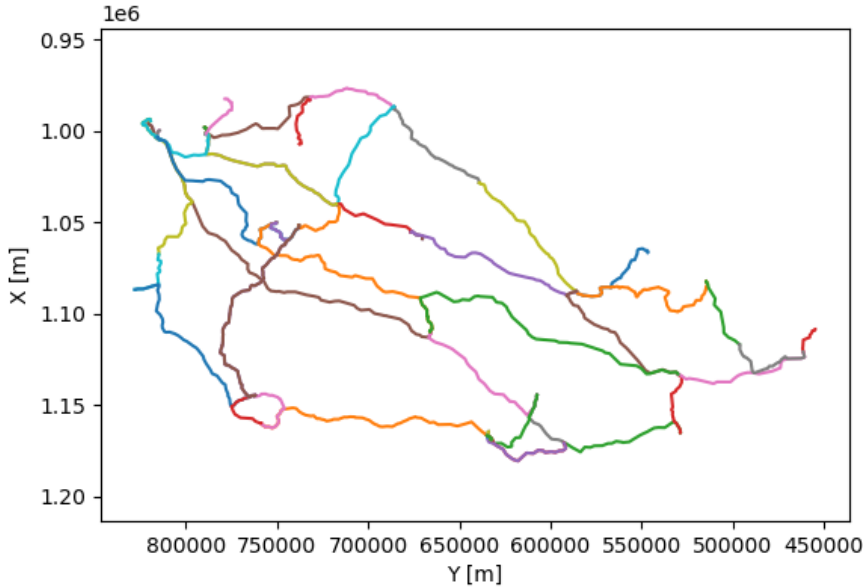


Figure 5.2: Plotted schema of Czech transmission grid

5.2 Grounding resistance of substation

This value is very difficult to obtain, because it is only measured during the transformer commissioning or during reconstruction. Unfortunately, only few values of grounding resistance for different substations were provided. Specifically for the following substations:

Substation	$R_i[\Omega]$
Čebín	0.031
Neznášov	0.090
Týnec	0.102
Tábor	0.272
Kočín	0.071
Prosenice	0.038

Table 5.1: Grounding resistances of substations that were provided by the ČEPS company

Remaining values for the substations where the grounding resistance of transformer are unknown and will be determined by estimation. The reference values are used as average of the known values, the sensitivity of the results to the choice of the values is tested in Section 8.1

5.3 Geoelectric field

Data of the geoelectric field were provided by the supervisor of this thesis in a text file. The calculation resulted from the code published within the master thesis of Tatiana Výboštková defended at Faculty of Mathematics and Physics, Charles University. For simplification it was assumed, that conductivity of the Earth only varies with depth and the approximation by the plane wave was used. From the values of magnetic field and the conductivity of the Earth the geoelectric fields components E_x and E_y were calculated. [36]

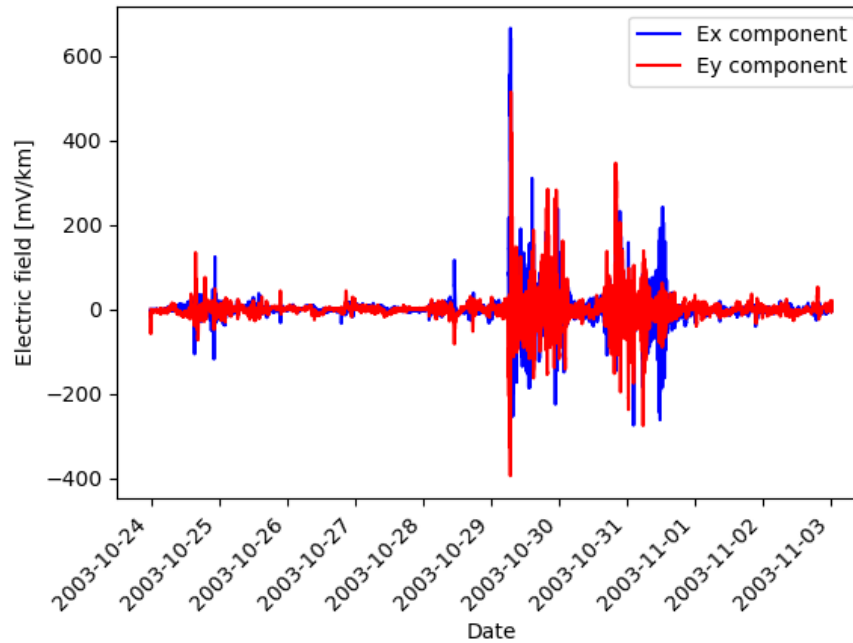


Figure 5.3: Geoelectric field

The period of measurements is from the 23rd October of 2003 to 1st of November of 2003. This corresponds to the period of the Halloween storms, that have affected all the world. The most significant consequences of this storm were tracked in Denmark and Sweden. Power grid systems of these countries was affected by the GICs that lead to blackout, that lasted for an hour. This event was mentioned in previous chapter.

5.4 Resistivity and length of the transmission lines

I obtained an Excel file from TSO - ČEPS, a. s., where for each transmission line of Czech power grid the total length of the line and its resistance and reactance was given. As mentioned before, for GIC calculation we only need to take into account the DC resistance, as GICs are considered to be direct current. If resistivity was provided, the resistance would be gained by multiplying the length and the resistivity of each transmission line.

There were also provided data of conductors used in the Czech transmission system, that could be used for calculating accurate resistivity of the transmission line. For our purpose, it is enough to calculate with the provided value of resistance and those data were not taken in account.

The longest transmission line in the Czech Republic was line V413, that was


divided in 2019 to two parts (transmission line V416 and V413), in Mírovka substation. Since then, the longest transmission line is line V420 from Hradec Východ to Mírovka substation.

5.5 Measured data from Mírovka substation

To validate this program and the model itself was used comparison of data calculated with the program and data that were measured in the transformer of Mírovka substation, which is located in the centre of Czech Republic and where 4 longest transmission lines leads to. Those data were provided by Ing. Pavel Mlejnek, Ph.D., from Czech Technical University in Prague, Faculty of Electrical engineering, who made and installed the measuring system in the Mírovka substation.

To measure the GICs was used sensor LEM HOP-800, that measured the current flowing through the middle conductor to the ground. The sampling frequency was set to 5000 Hz. The temperature was measured every 1 second. For our use we have a set of data resampled to 1 Hz.

The data were available for period of 10 March - 18 October 2018 and 13 March - 18 September 2019. For this thesis were provided data sets for every day of April 2019. To compare the obtained and the calculate values, three days of April 2019 were chosen. Due to the low solar activity during those days the values of GICs were low.



Chapter 6

Model implementation

After obtaining the data necessary for the model itself, the model was rewritten to a Python code for GIC calculation. The code can be divided into several parts, steps. The main steps are shown in Fig 6.1 and will be further described. This program can be used for any transmission system that is described with parameters described in previous chapters for any time period, that the geoelectric field data are available for. The time evolution is solved by loops to following time value (according the geoelectric field).

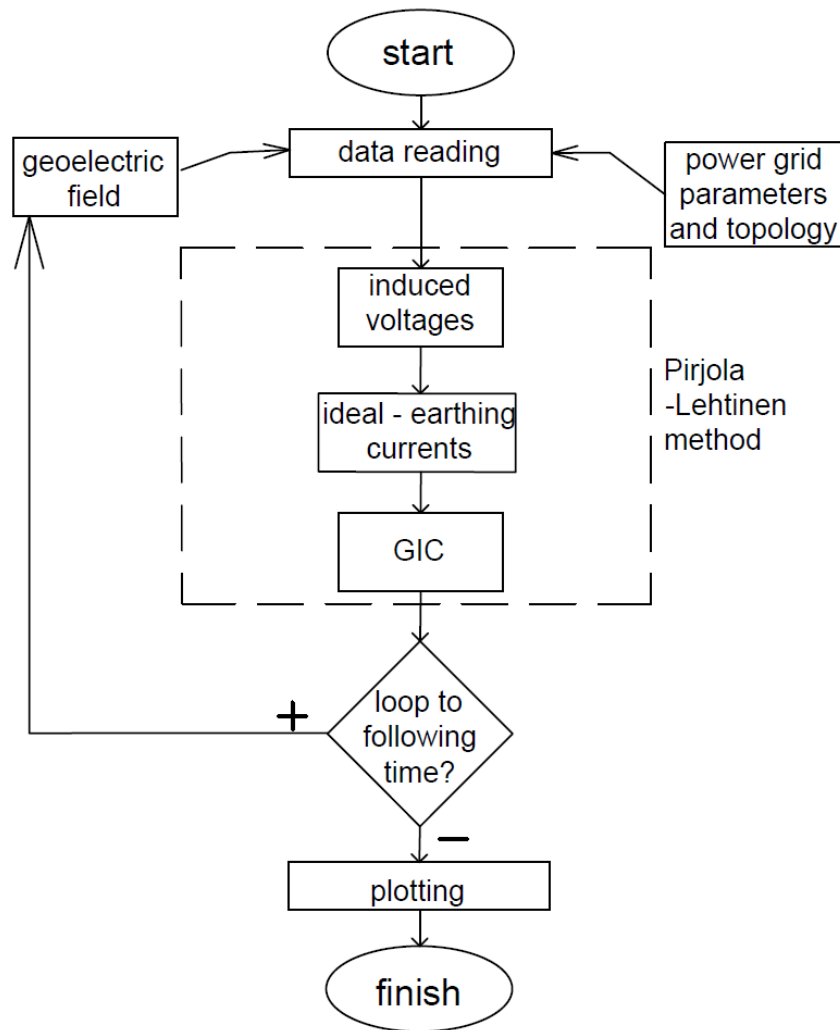


Figure 6.1: The flowchart of the code

6.1 Data reading

First of all, the program checks, if all data necessary are available. If not, the program cannot run and then ends with a error message. Otherwise, if all data are available, the program read and save data from the files to suitable structures. Mostly, the structures used in this code were Python dictionaries, which keys were usually transmission lines or substations.

Some of the input parameters had to be converted to a different structure than the structure that was available. For example, for line resistance, had to be taken into account, that the lines are multiple conductors or for coordinates, that the values are in meters and the axes are reversed.

■ 6.2 Induced voltages

The input for induced voltage calculation is geoelectric field, line coordinates and line resistance. According to Lehtinen-Pirjola method 4.3, the induced voltage was calculated, plotted and saved to a excel file and a dictionary for all transmission lines included in this system. The dictionary is input for another step following the induced voltage calculation.

■ 6.3 Ideal-earthing currents

The input for ideal-earthing current is induced voltage and it was again calculated according to Lehtinen-Pirjola method with equation 4.2 for all transmission lines leading to this substation and its resistance. The output is calculated, plotted and saved to a excel file and a dictionary for all transmission lines included in this system.

■ 6.4 GIC

The input for the final calculation of GIC is ideal-earthing currents, impedance and admittance matrix describing the transmission line structure. The equation used is again from the Lehtinen-Pirjola method, see 4.1. The output is calculated, plotted and saved to a excel file and a dictionary for all substations included in this system.

Chapter 7

Results

7.1 Halloween storms

One of the main aims of this thesis was to model GICs for the event of Halloween storms, that was mentioned in previous chapters. This period is special because it was connected with the registered effects on power grids worldwide. The term “Halloween storms” denotes a period of a disturbed geomagnetic field that persisted for several days at the end of October and beginning of November 2003. This storm is often studied in analyses similar to the one used this thesis, therefore it was only natural to focus to this period.

As already mentioned, the horizontal components of the geoelectric field was given to me as a result of the previous project [36] in a form of a sequence of stationary models with a 1-minute cadence. For each time instance was independently computed the modelled GICs at the nodes of the ČEPS, a.s., power transmission grid by my own program. The resulting sequences of the modelled GICs in time are presented mostly in the form of the plots with the time being the independent variable. The plots were generated by the program for all of the substations included in the transmission grid, but only few of them will be shown in this thesis. As mentioned before, the GIC amplitude depends on the grounding resistance of transformer in the substation, on the geoelectric field, on ground resistivity, on the line length and on the line resistivity.

7.1.1 Geomagnetic voltage

First, from the knowledge of geoelectric field components, line coordinates and line parameters, the geomagnetic voltage for each substation was calculated and modelled using equation (4.3) mentioned in this thesis. The geomagnetic voltage values mainly depend on the line length and its orientation on Earth surface.

In the table 7.1 are all calculated geomagnetic voltages, for all transmission lines that are included in this studied system. It is clear, that lower values of

line	length [km]	maximum V [V]	line	length [km]	maximum V [V]
V400	46.2	31.9	V453	84.1	55
V401	103.8	70.9	V454	67.6	36.3
V402	87.6	52.1	V457	59.8	31.5
V403	79.6	47.6	V458	107	47.3
V405	53.5	24.7	V459	42	23.4
V410	95.4	60.3	V460	16.5	8
V411	45.4	17.6	V461	11.1	5.5
V412	116.9	58.9	V462	11.1	5.5
V413	145.1	75.7	V463	4	2.2
V414	29.5	8.6	V464	4	2.2
V415	35.1	16.8	V465	19.2	5.5
V416	184	98	V466	19.2	5.4
V417	74.1	42.5	V467	4.3	1.7
V418	37.7	16.1	V468	4.3	1.7
V419	95.4	60.3	V469	4.5	1.8
V420	209.6	134.7	V470	30.8	13.8
V422	88.4	50.2	V471	8.8	5.3
V423	38.3	18.5	V472	8.8	5.4
V430	82.2	32.7	V473	35.6	7.4
V431	32.6	14.3	V474	42.9	7.4
V432	115.9	63	V475	137.7	51.7
V433	142.7	84.5	V476	129	54.2
V434	50.7	24.2	V480	28.9	12.6
V435	55.6	29.5	V481	2.3	1.2
V436	55.6	29.3	V482	2.3	1.2
V450	72.3	42.3	V483	3.3	1.7
V451	53.6	32	V484	3.4	1.8
V452	68.3	44.5	V485	3.5	2.1
			V486	3.7	2.2

Table 7.1: Geomagnetic voltage for all transmission lines

geomagnetic voltage are for shorter lines, which have lower resistance. In the figures below few examples of calculated geomagnetic voltage for transmission lines are displayed. They represent two longest and two shortest lines of the Czech transmission system to give a feeling of the maximum and minimum induced voltages. It is evident, that for lines V414 and V415 which both are quite short – around 30 km and have very low resistance, the geomagnetic voltage is very low compared to values shown for lines V416 and V420 which are 184 km and 209.6 km long. That confirms, that the parameter, which matters the most in case of geomagnetic voltage calculation, is the line length.

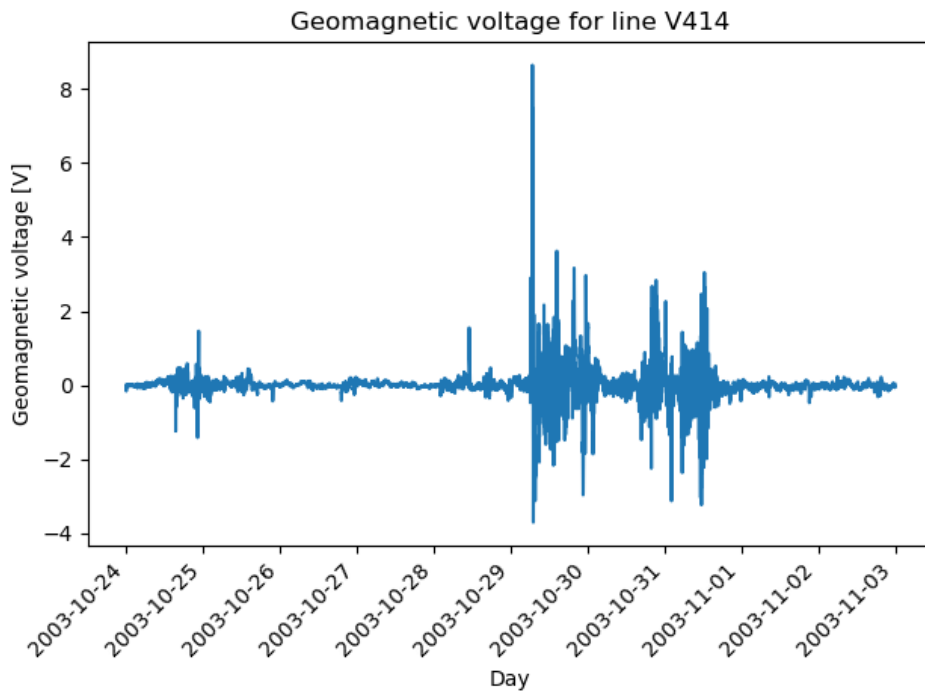


Figure 7.1: Geomagnetic voltage for the line V414

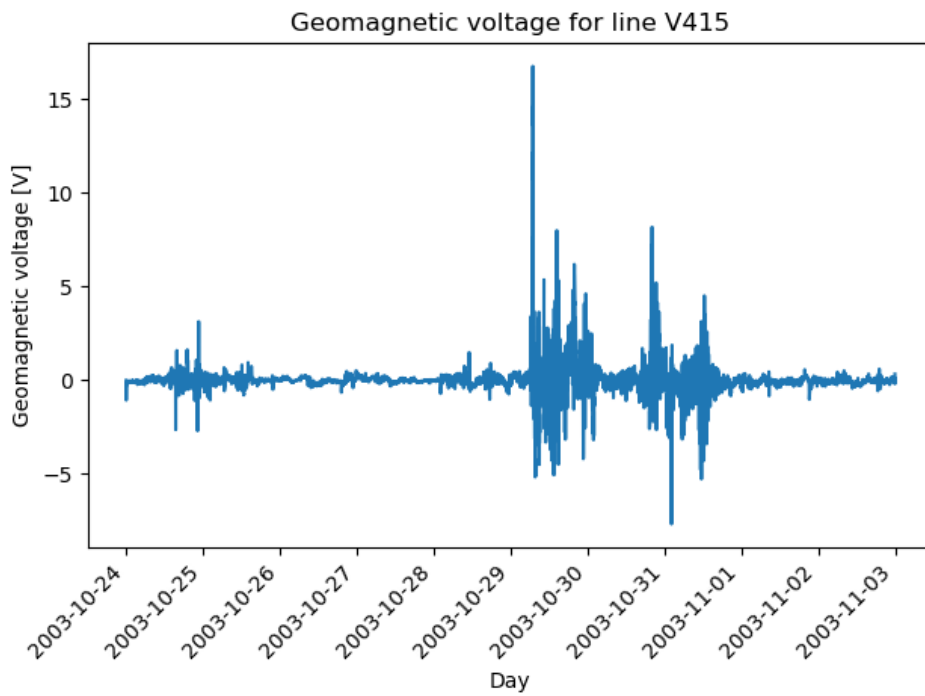


Figure 7.2: Geomagnetic voltage for the line V415

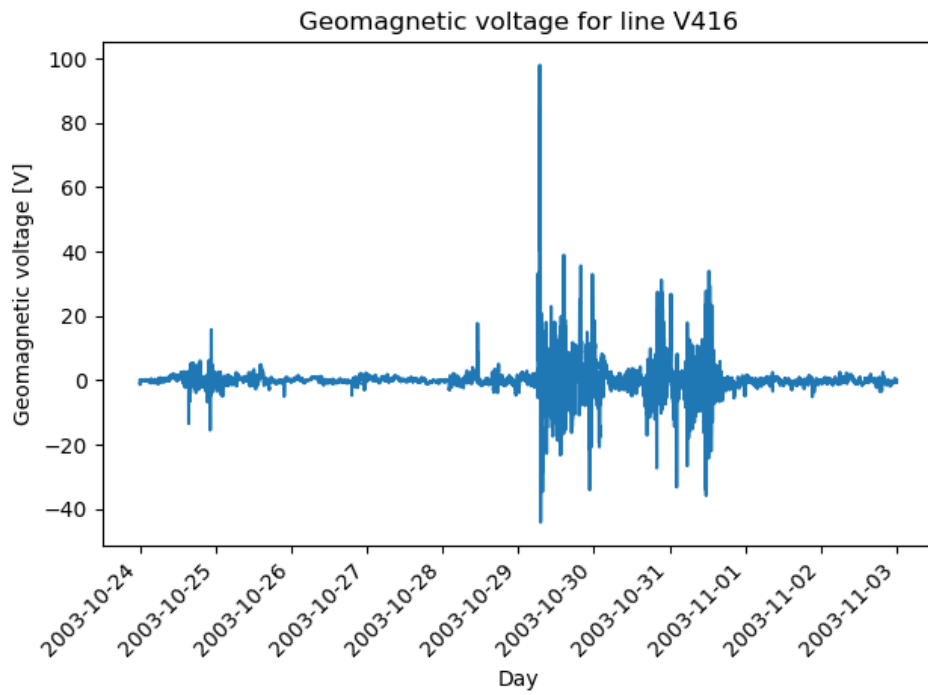


Figure 7.3: Geomagnetic voltage for the line V416

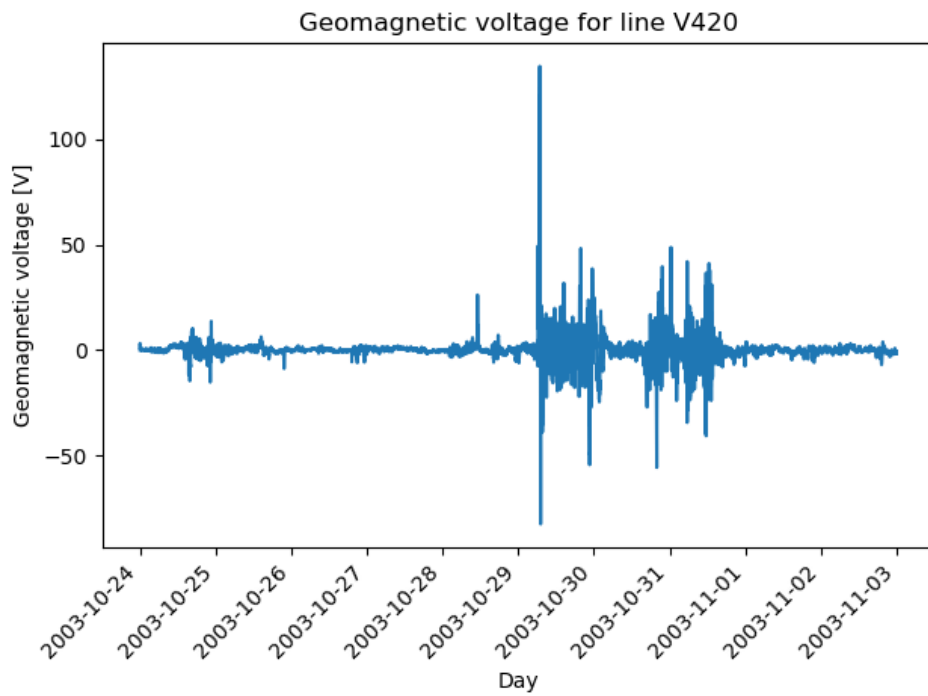


Figure 7.4: Geomagnetic voltage for the line V420

7.1.2 GIC

The dataset kindly provided by ČEPS, a.s., contained the grounding resistances for only a handful substations. For the remaining I chose the average value of the provided resistances to obtain the reference solution of the electrical circuit and the GICs. The sensitivity of the solution to this choice will be discussed later. The GIC amplitudes of the reference solution for the period of Halloween storms in 2003 are shown in figures below for a few selected stations. The maximum and minimum values for rest of the substations in the Czech transmission system are given in table 7.2. In this chapter some details are explained about the chosen substations and the amplitudes of the GIC is these substations. I would like to point out that the maximum values modelled for the Halloween storms period in the Czech Republic is in a very good agreement with the maximum GIC modelled for the same period for the Austrian Power Grid [24]. Their maximum was 13.38 A.

Substation	GIC [A]		Substation	GIC [A]	
	min	max		min	max
Albrechtice	-7.9	3.9	Mírovka	-16.0	8.8
Babylon	-8.9	3.9	Mělník	-5.6	10.9
Bezděčín	-15.0	7.3	Neznášov	-17.3	11.3
Chodov	-10.4	5.8	Nošovice	-2.9	6.7
Chotějovice	-10.7	5.2	Otrokovice	-7.1	10.2
Chrást	-5.7	12.6	Počerady	-5.9	9.1
Chvaletice	-3.6	2.5	Prosenice	-8.7	8.1
Dalešice	-3.6	7.6	Pruněrov I	-8.9	7.1
Dasný	-2.4	3.6	Pruněrov II	-3.7	3.4
Dlouhé Stráně	-17.3	8.0	Přeštice	-16.6	12.5
EDU I	-2.8	6.5	Slavětice	-3.0	6.4
EDU II	-2.8	6.5	Sokolnice	-4.9	11.7
Horní Životice	-11.7	14.9	Tušimice II	-1.1	2.2
Hradec Východ	-1.6	2.2	Týnec N/L	-1.6	3.7
Hradec Západ	-0.9	0.5	Verněřov	-8.1	9.7
Kletné	-12.7	10.8	Výškov	-4.9	8.6
Kočín	-3.6	8.3	Čebín	-15.3	7.2
Krasíkov	-4.1	9.8	Čechy Střed	-4.7	9.7
			Řeporyje	-12.6	7.2

Table 7.2: GIC values for Halloween storm 2003

Bezděčín substation is substation where 5 transmission lines are connected, 3 of them are voltage level of 400 kV (V451 with a total length of 53.6 km, V452 totally measuring 68.3 km and V454 with a length of 67.6 km). This substation is located on the North-West of the country. To this substation, the power plant Ledvice is connected. The maximum value of GICs calculated for Halloween storm for this substation is 7.3 A and minimum is -15.3 A.

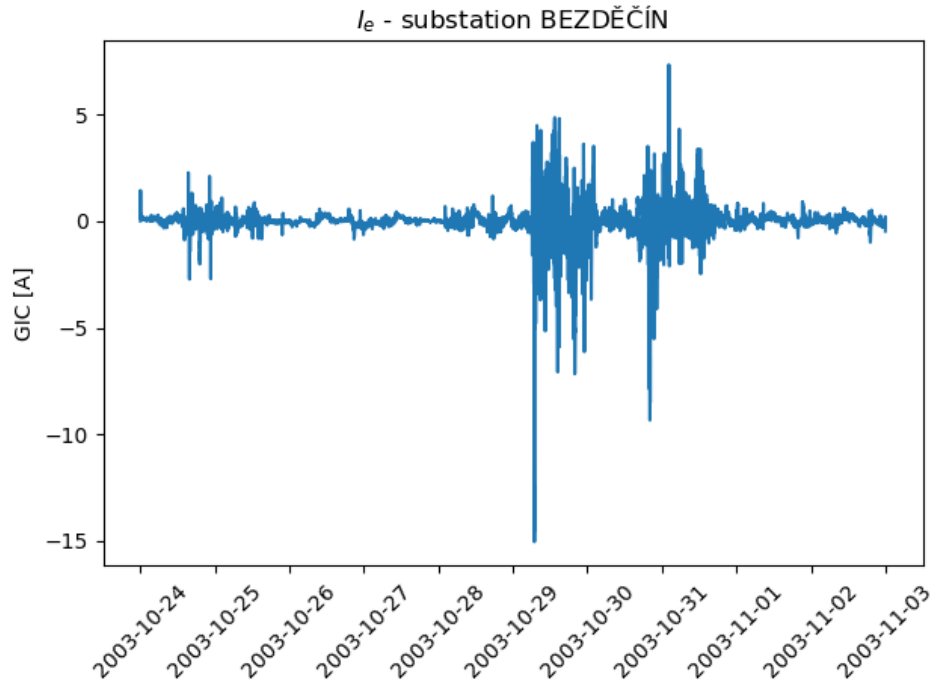


Figure 7.5: GIC for Bezděčín substation - Halloween storms 2003

For this substation we can say, that the amplitudes of modelled GICs have average values among the others under study.

Dlouhé Stráně substation is substation on the North-East of the country, where is only one line connected – the pumped-storage hydroelectric power station Dlouhé Stráně. The length of the V457 transmission line from Dlouhé Stráně to substation Krasíkov is 59.8 km. Maximum of GICs in Dlouhé Stráně substation is 8 A and minimum -17.3 A. The amplitudes for this substation are comparable to values for the Bezděčín substation, as the length of the line leading to this substation is very similar.

Mírovka could be considered as the main substation in the Czech Republic, as it is in the centre of the country and where leads the longest transmission lines in the Czech Republic. In this substation there are four 400 kV transmission lines (V413 – 145.1 km, V416 – 184 km, V420 – 209.6 km and V422 – 88.4 km). The amplitudes calculated for this substation are a bit larger then for the previous substations, as the length of the lines leading to this substation are longer.

Tušimice is another power plant in the Czech Republic with own substation. From this substation two transmission lines lead, that are both quite short, V463 – 4km and V464 – 19.2 km, those lines lead also to the substation Hradec Zapad, as these lines connect these substations. For Tušimice substation

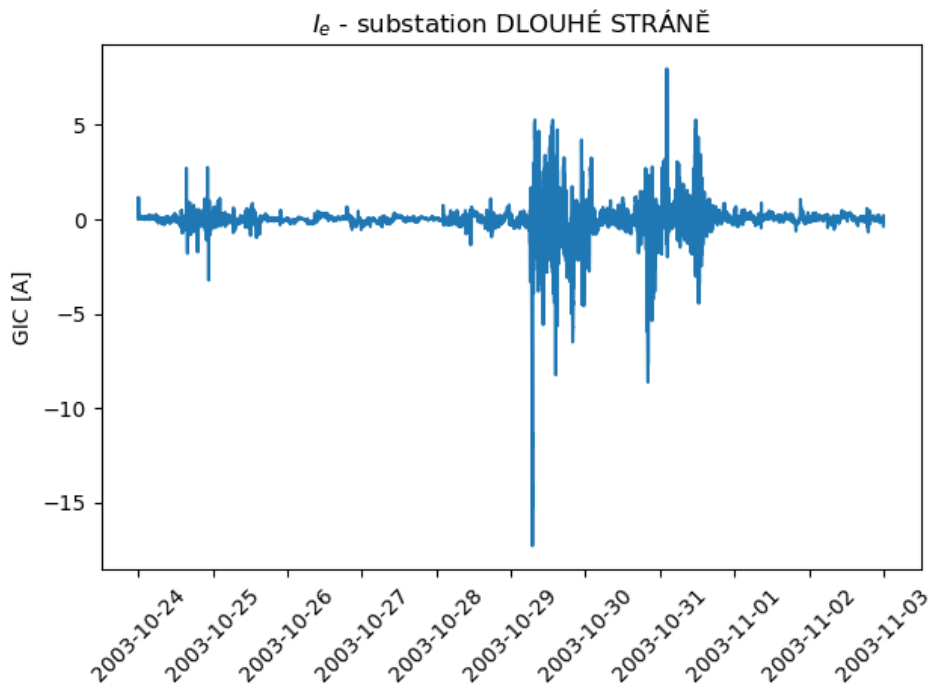


Figure 7.6: GIC for Dlouhé Stráně substation - Halloween storms 2003

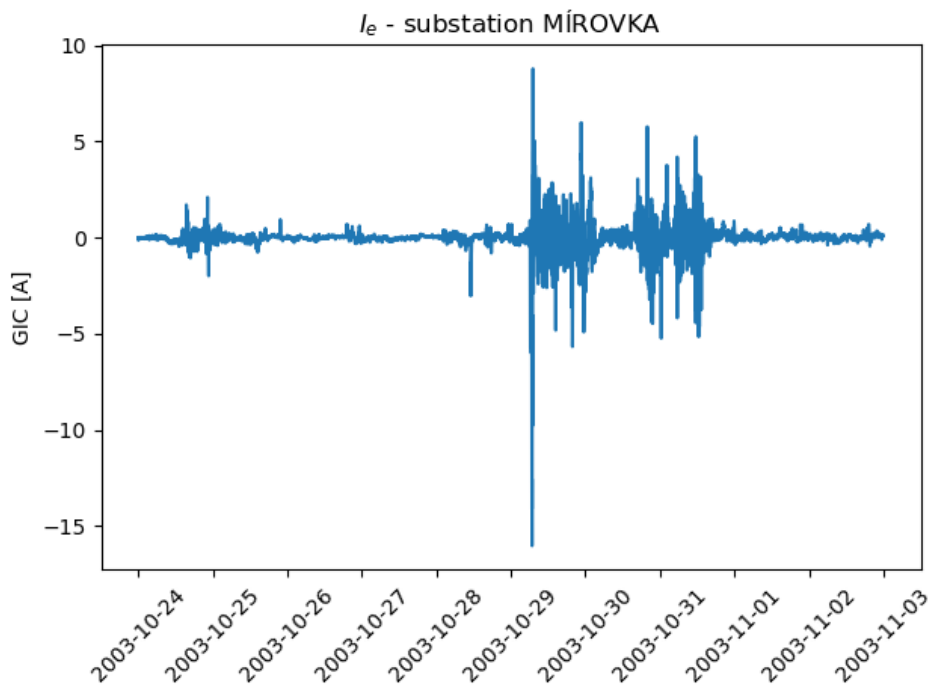


Figure 7.7: GIC for Mírovka substation - Halloween storms 2003

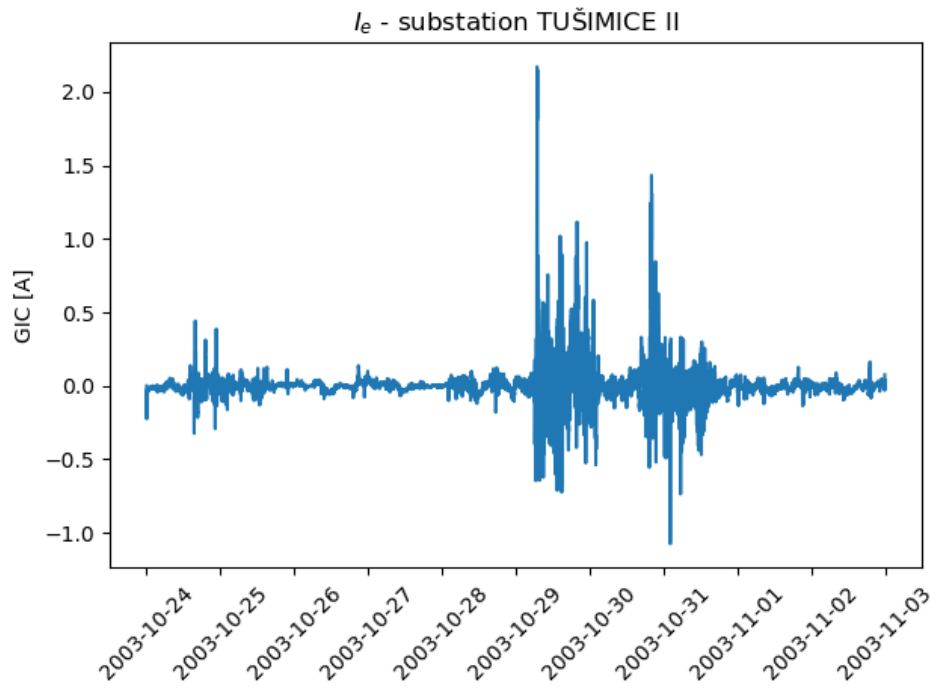


Figure 7.8: GIC for Tušimice substation - Halloween storms 2003

we can notice, that the values of modelled GICs are much lower, then for the previously shown substations. The length of the lines leading to this substation is, comparing with the previous, much shorter.

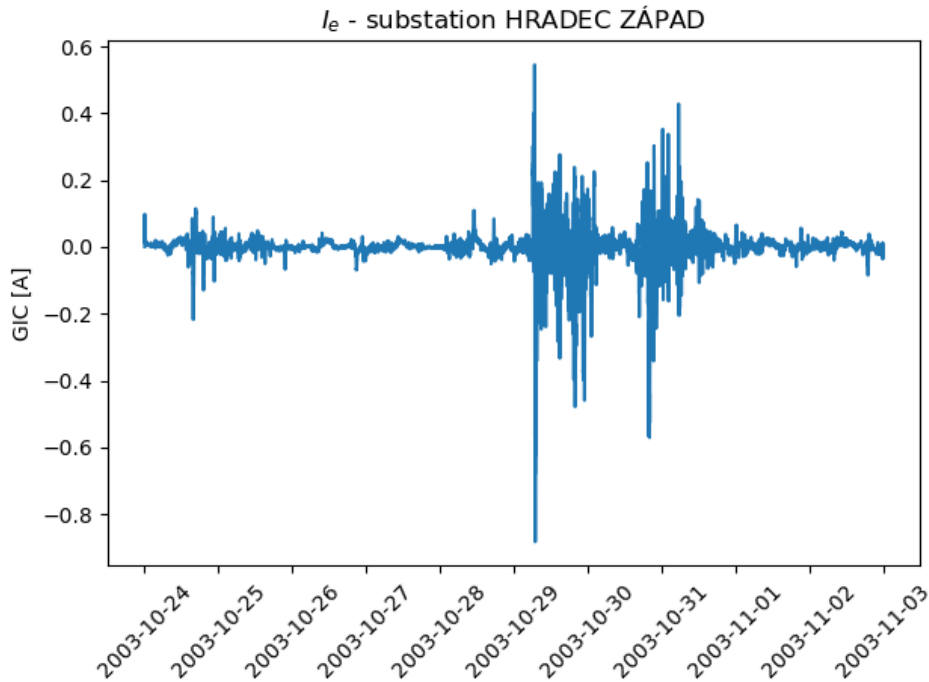


Figure 7.9: GIC for Hradec Zápád substation - Halloween storms 2003

Hradec Zápád is a part of a substation Hradec u Kadaně, located in the West part of the Czech Republic, the number of transmission lines leading to this substation is 6. The two transmission lines mentioned in previous paragraph, V463 – 4km and V464 – 19.2 km and V465 – 19.2 km, V466 – 4.2 km, V411 – 45.4 km and V412 – 116.9 km. The small values calculated for this substation might be caused by compensating current induced from one substations between each other and also quite short transmission lines leading to this substation.

7.2 Geoelectric field of 1 V/km

During Halloween storms the geomagnetic field was disturbed quite strongly and for a long time. This long-lasting period of the geomagnetic storms is considered one of the strongest in recent years. In order to obtain the reasonable estimates of the GIC amplitudes that could possibly be expected in the Czech transmission network, I computed the GIC model for the geoelectric field of the amplitude of 1 V/km. This value is attributed to an extreme geomagnetic storm. Note that during the Halloween storms, the peak magnitudes of the geoelectric field was about 650 mV/km, that is about a half of the chosen extrem value.

In table 7.3 the GIC values in the grid nodes are given for this reference extreme value. We can expect the highest values for substation Přeštice

(42.4 A) and Řeporyje (−40.7 A), which are both big substations in the Czech Republic, where the longest transmission lines leads. The lowest GIC amplitudes calculated are for substations, that are compared to the substations with higher amplitudes small and lines leading to those substations are shorter - for example substation Hradec Západ, Tušimice II and Týnec N/L, where the amplitudes are in orders of units of Amperes.

substation	GIC [A]	substation	GIC [A]	substation	GIC [A]
Albrechtice	−22.7	Hradec Východ	18.5	Prunéřov II	−18.3
Babylon	−30.7	Hradec Západ	2.7	Přeštice	42.4
Bezděčín	−32.8	Kletné	−28.8	Slavětice	−15.2
Chodov	−33.8	Kočín	23.5	Sokolnice	23.4
Chotějovice	30.3	Krasíkov	32.9	Tušimice II	−7.6
Chrást	39.8	Mírovka	−34.7	Týnec N/L	−7.7
Chvaletice	12.3	Mělník	30.8	Vernéřov	27.2
Dalešice	−19.8	Neznášov	29.7	Výškov	−26.6
Dasný	−19.8	Nošovice	17.6	Čebín	−39.4
Dlouhé Stráně	−36.5	Otrokovice	−25.2	Čechy Střed	20.0
EDU I	−21.1	Počerady	−28.4	Řeporyje	−40.7
EDU II	−21.0	Prosenice	27.1		
Horní Životice	30.1	Prunéřov I	−23.7		

Table 7.3: GIC values for geomagnetic field value 1 V/km

Chapter 8

Discussion

8.1 Effects of the unknown earthing resistances

In the Pirjola-Lehtinen model, the GIC (the current flowing between the Earth and the node) amplitudes depend on the values of the earthing resistances, see equation (4.1). Unfortunately, in the case of this thesis, the grounding resistances were known only for a few substations (see Table 5.1). For the remaining substations, I chose the average of the values given in Table 5.1, that is 0.1Ω .

Since the solution depends on the chosen value, I tested its sensitivity on the value chosen. Apart from the reference solution I thus computed two more solutions for the unknown grounding resistances having the maximum value of the known ones (that is 0.272Ω) and the minimum value from the known one (that is 0.031Ω). One may assume that the unknown grounding resistances of the remaining substations will not be far from this minimum–maximum range. The respective solutions hence consist of the minimum and maximum GIC values for the period of Halloween storms.

The sensitivity was tested by comparing the GIC values for the two supplementary solutions with the reference solution. The differences for three selected substations are given in the figures below.

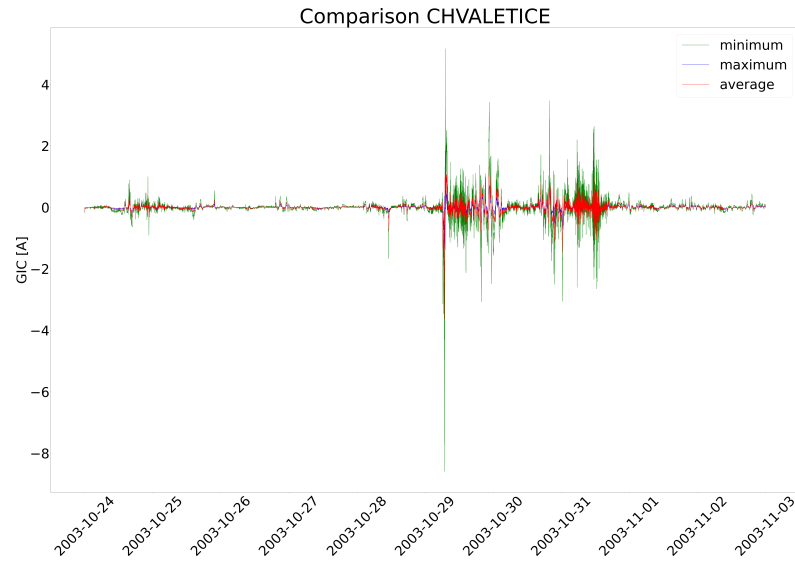


Figure 8.1: Calculated GIC for Chvaletice substation for different grounding resistances

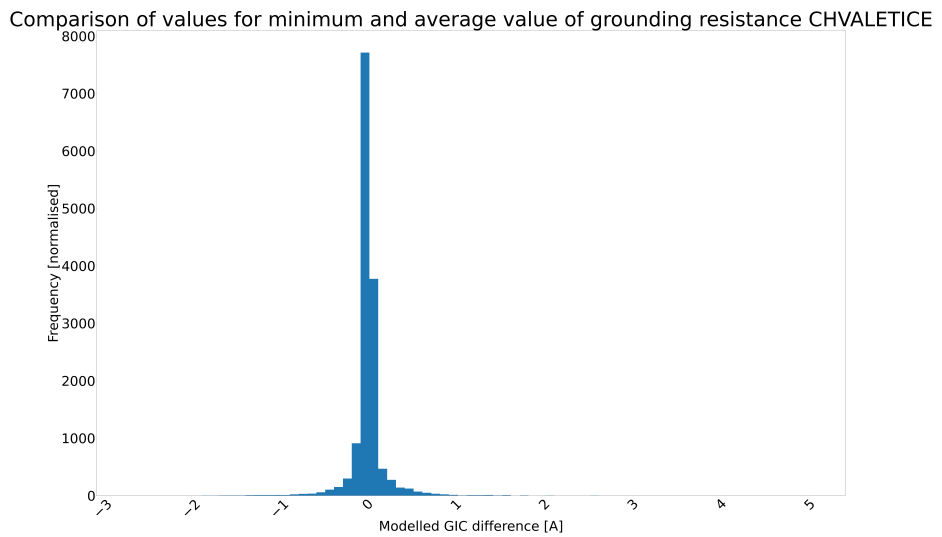


Figure 8.2: Histogram of differences in results for minimum and average resistance for Chvaletice substation

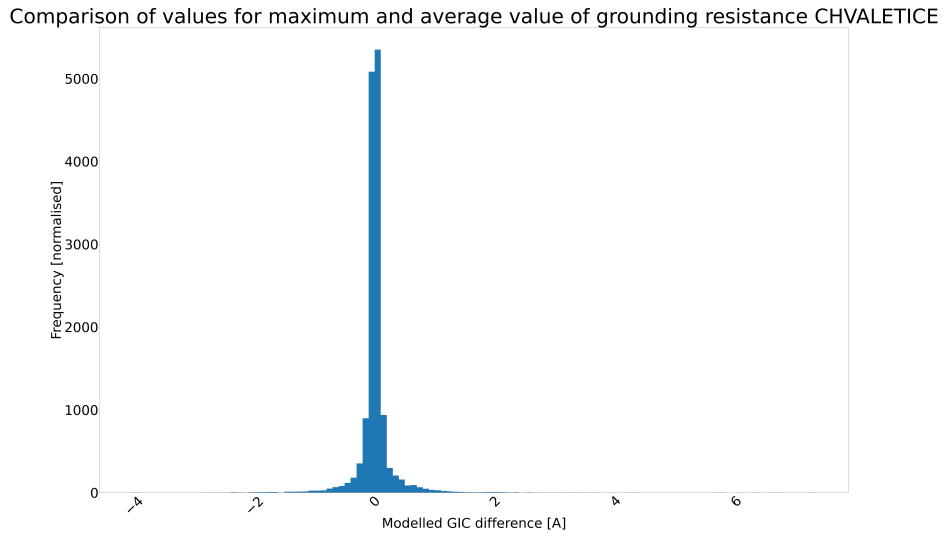


Figure 8.3: Histogram of differences in results for maximum and average resistance for Chvaletice substation

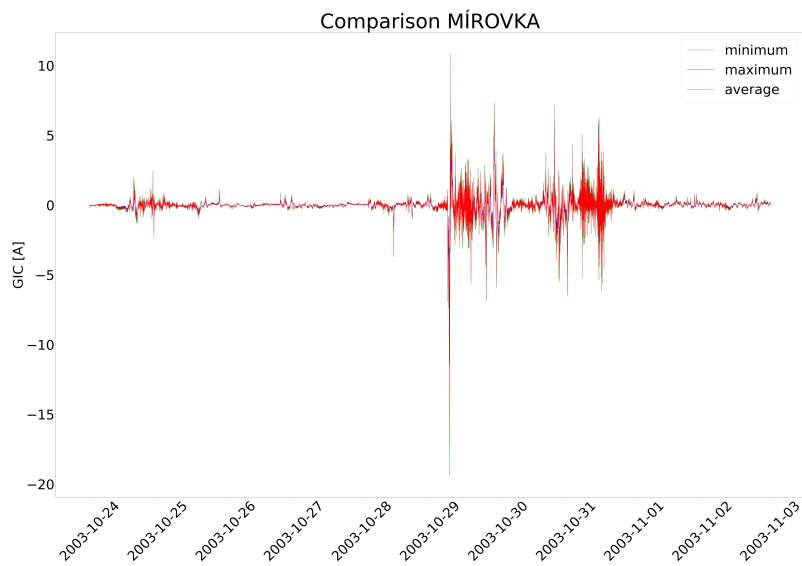


Figure 8.4: Calculated GIC for Mírovka substation for different grounding resistances

Comparison of values for minimum and average value of grounding resistance MÍROVKA

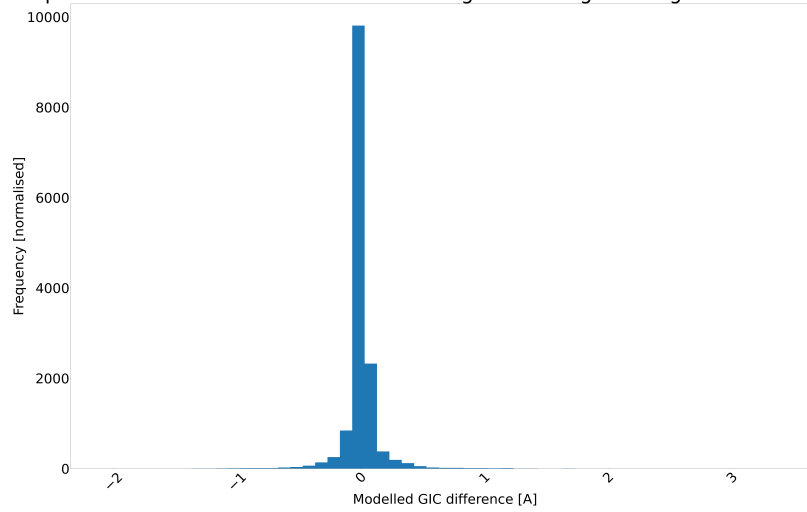


Figure 8.5: Histogram of differences in results for for minimum and average resistance for MÍROVKA substation

Comparison of values for maximum and average value of grounding resistance MÍROVKA

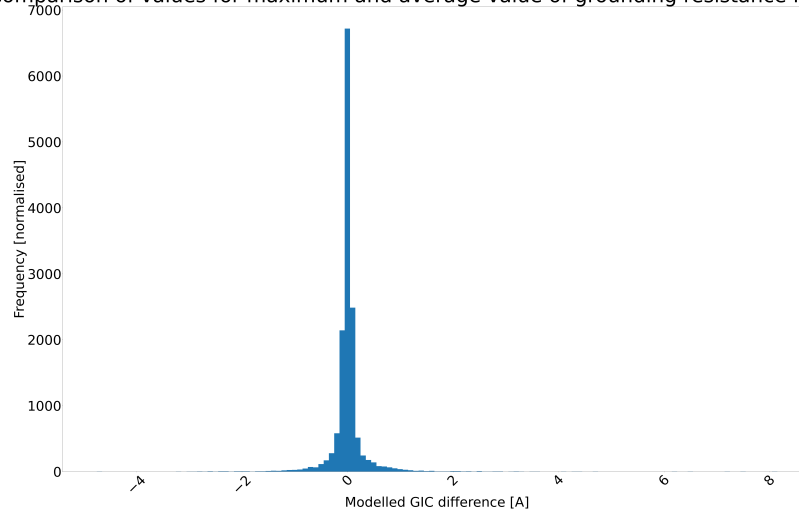


Figure 8.6: Histogram of differences in results for for maximum and average resistance for MÍROVKA substation

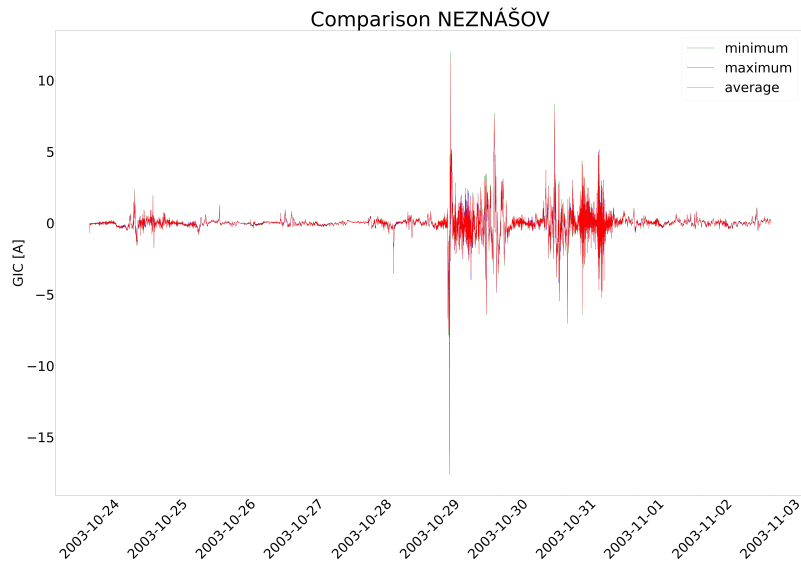


Figure 8.7: Calculated GIC for Neznášov substation for different grounding resistances

Comparison of values for minimum and average value of grounding resistance NEZNÁŠOV

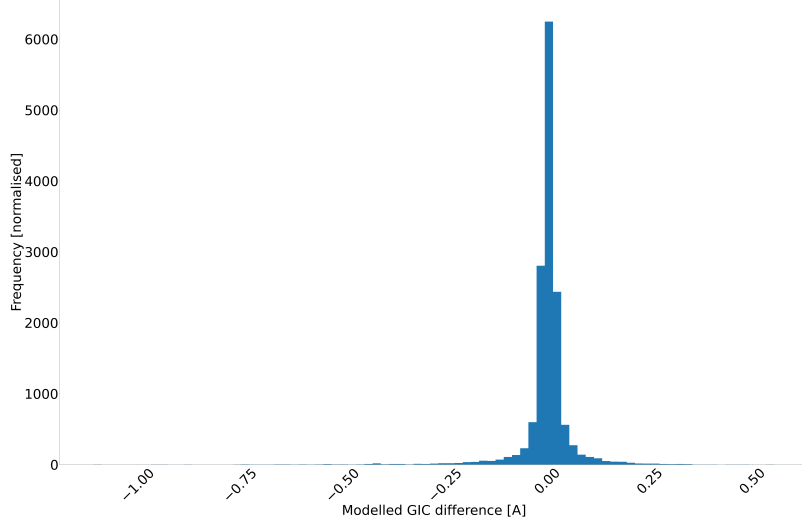


Figure 8.8: Histogram of differences in results for minimum and average resistance for Neznášov substation

Comparison of values for maximum and average value of grounding resistance NEZNÁŠOV

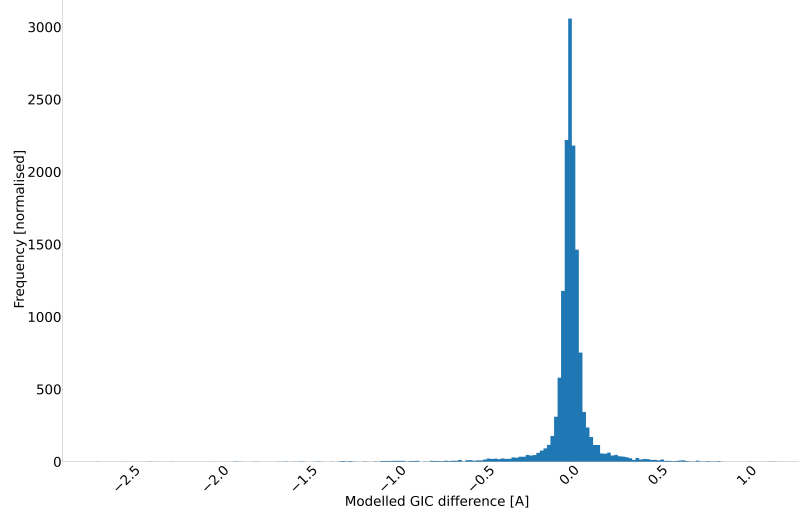


Figure 8.9: Histogram of differences in results for maximum and average resistance for Neznášov substation

From the results of graph comparisons there are shown three chosen substations. We can see, that there is a difference for calculated values of GIC for different grounding resistance. From the graphs is evident, that for lower grounding resistance value, the calculated GICs are higher than for higher values of grounding resistance. For example for substation Neznášov (for which the grounding resistance was obtained from TSO) we can see that all three time evolutions are almost equal, the differences are much less than 10 per cent. From the histograms it comes clear that over the period of Halloween storms, the differences between the solutions when using various values of earthing resistance are most often below 0.1 A. This indicates that the GIC amplitude computed for the substation with a known grounding resistance depends only weakly on the grounding resistances of the other nodes in the power grid.

On the other hand, for substations Mírovka and Chvaletice with unknown grounding resistance the differences are more significant. The GIC amplitudes may consequently be different even by 50 per cent or more in some peaks and to the first approximation they are inversely proportional to the grounding-resistance value. The histograms of the differences between the different solutions are considerably wider than in the case of Neznášov substation. Still, the histograms are strongly peaked around the bin with the value of the difference less than 0.1 A, hence the solutions using different earthing resistances are still somewhat comparable.

The conclusion from this sensitivity analysis is, that for more precise results of GIC it is necessary to know all grounding resistances of the substations

included in the conductor system.

8.2 Validation to measured data

The modelled GIC should be directly validated against the real measurement. The only real GIC measurements were performed using a device installed in Mírovka substation. For the purpose of this thesis I obtained the data covering each day of April 2019.

For the same period for which we have available data from the measurements, the GICs are modelled. The period of one month, that was available, was divided into days, so its easy for us to compare the results. The plots of the modelled and measured GIC for a few chosen days are displayed in figures below.

Unfortunately, the comparison is very inconclusive. From the whole month only on three days the modelled and measured GIC had magnitudes of the same order. On the remaining days that values of the measured GICs were very large with jumps to values even of the order of tens of amperes for a very long time. These measurements cannot be due to the geomagnetic activity, because it was very low during the whole April 2019. The sources of the high-amplitude peaks and other jumps are different and unknown to me.

For the three days of 27th, 28th and 29th April at least the amplitudes were of a similar order. These days are plotted below. We see that the measured GICs are systematically shifted towards negative values, whereas the modelled GICs are only slightly varying about zero. It is very hard to speak about a correlation between these two series. Visually, one can notice that on days 27th and 28th of April, in the first half of the day the trends in both curves are somewhat similar. In the second half this similarity breaks. A similar conclusion might be applicable also for the day 29th of April, however it is even less evident.

An overview plot of both the measured and modelled GICs in Mírovka substation over the whole tested month is given in Fig. 8.14. One can see that whereas the modelled GIC oscillate around the zero value and are well below 1 A in their amplitudes over the whole month, the measured GIC reach very large values in the peaks and show increased values of tens of amperes persisting over many hours or even days. As a reference series for comparison I also plotted the geomagnetic K index in the same time period, which is given in the bottom panel of Fig. 8.14.

The K index is a semi-logarithmic quantity describing changes in the amplitude of the horizontal component of the geomagnetic field over a three-hour interval. K index method defines irregular variations as the range (difference)

between the upper and lower values. The values of $K < 5$ in quiet, $K > 5$ indicate the storm and $K = 9$ indicates the superstorm. Derivation of K index depends on the geographic location of the observatory. In practice, observatories at higher geomagnetic latitude require higher levels of fluctuation of the geomagnetic field for a given K index. The K displayed in the bottom panel of Fig. 8.14 was calculated by my supervisor using a Finnish Meteorological Institute method [37], with a limit of 500 nT for $K = 9$ utilising the geomagnetic field measurements from the Czech geomagnetic observatory Budkov, which are freely available via the Intermagnet.org portal.

During the whole April 2019, the geomagnetic field showed only minor fluctuations with no indication for the ongoing geomagnetic storm. Therefore, it is highly unlikely, that the large currents measured by the sensors installed at Mírovka substation are of the geomagnetic origin, namely they cannot be because of the GICs flowing in the transmission network.

At this point I unfortunately have to conclude that the measured GICs suffer from the sources of the unknown origin and that the comparison to the model is not possible. The proper understanding what were the components of the currents measured in Mírovka substation is beyond the scope of this thesis.

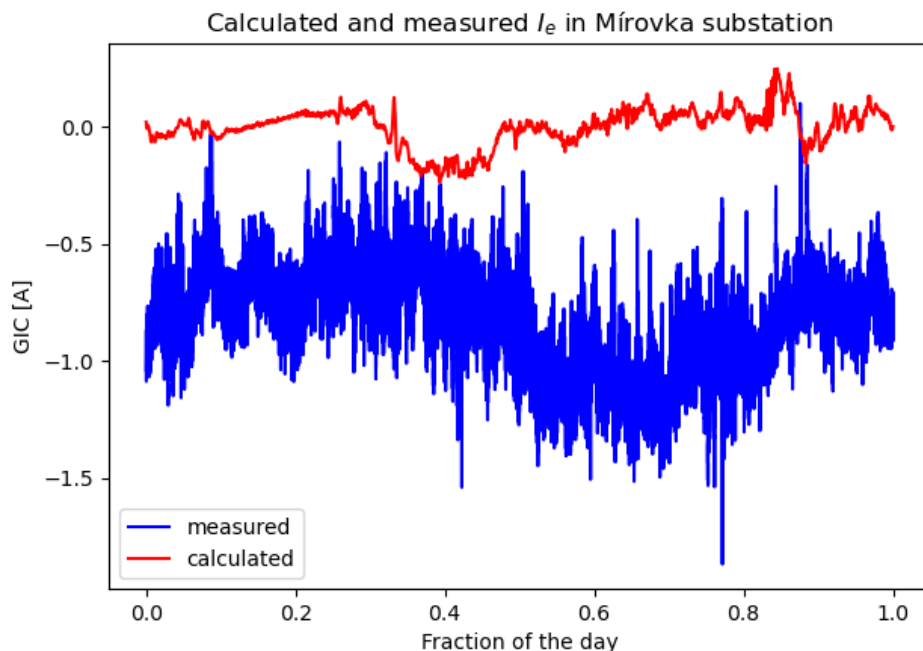


Figure 8.10: Comparison of calculated and measured GIC for 27th April 2019

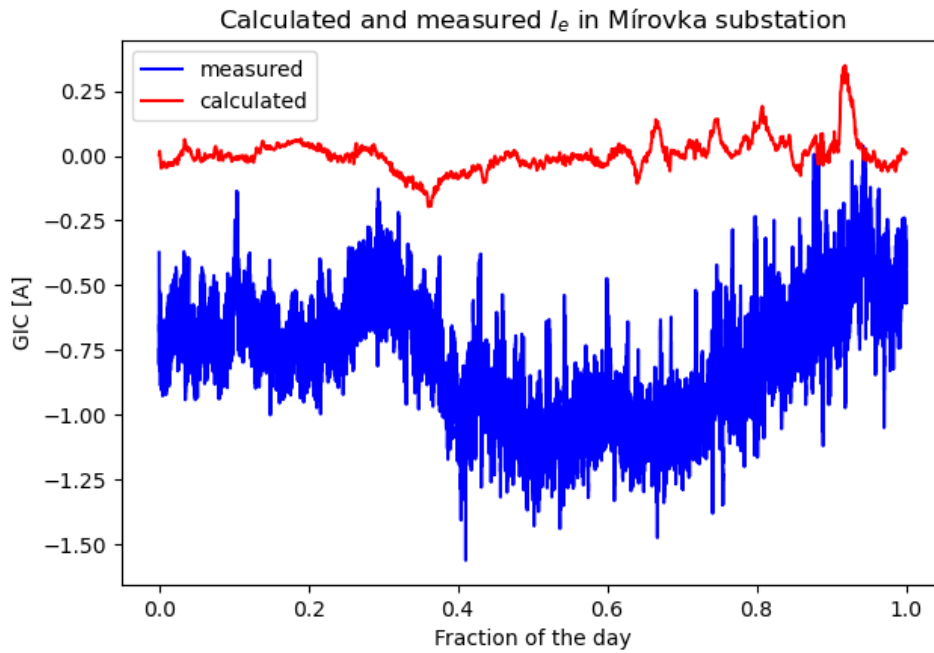


Figure 8.11: Comparison of calculated and measured GIC for 28th April 2019

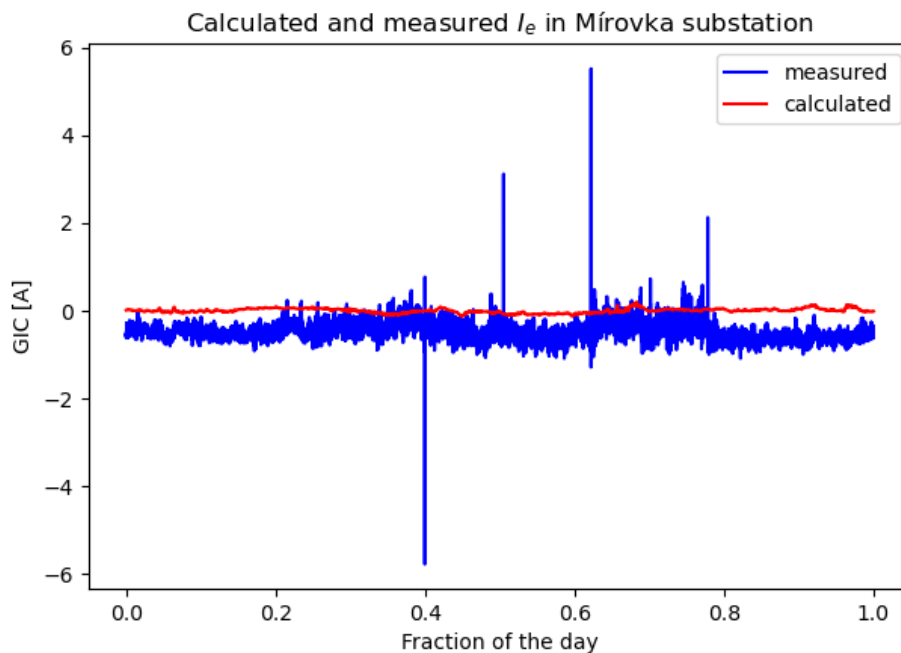


Figure 8.12: Comparison of calculated and measured GIC for 29th April 2019

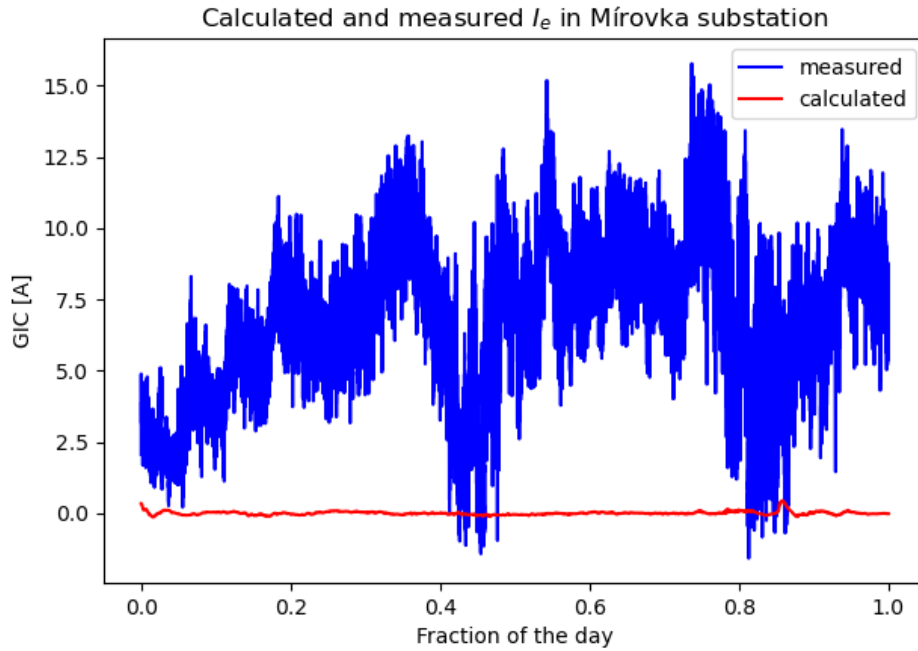


Figure 8.13: Comparison of calculated and measured GIC for 13th April 2019

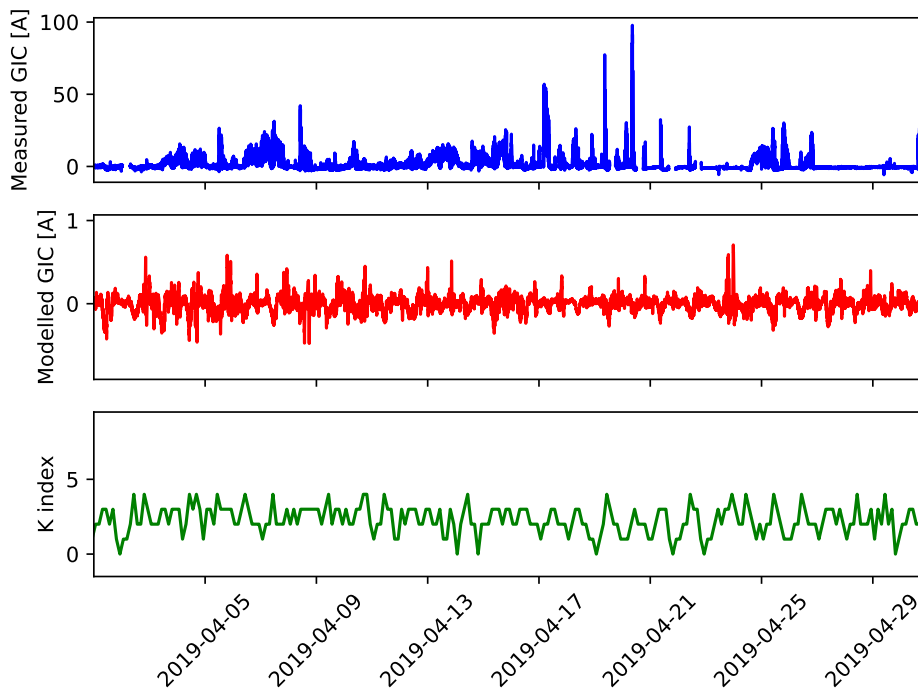


Figure 8.14: Comparison of the measured GIC, modelled GIC in the Mirovka substation over the whole month of April 2019 with the overall geomagnetic activity represented by the K index.

Chapter 9

Conclusions

The main aim of this thesis was to determine the expected values of GICs for the event of Halloween storm for Czech transmission system. Based on the calculation using Lehtinen-Pirjola method, it can be concluded, that values for this event of Halloween storm were in the order of units of amperes, which are much lower compared to values measured in Scandinavia during the Halloween storm (calculated peak value 330 A), which caused blackout or compared to values that caused blackout in 1989 in Quebec. Even when those amplitudes do not reach values that could cause immediate destruction, in a longer term, when the power grid components are exposed those currents, we could expect problems associated with the GICs, such as increased rate of anomalies that will probably be classified as “aging”. As mentioned, the Czech Republic and Austria are bordering countries, that are both located in mid-latitude area and the results from these countries could be compared. The maximum calculated value for Austria was 13.38 A, which is very similar to values calculated for the Czech Republic.

Another step was calculation values for event of extreme geomagnetical storm, which could be expected to happen in the area of the Czech Republic. For this event, the amplitudes were higher, in orders of tens amperes with a maximum of about 40 A predicted for the substations, where the longest transmission lines connect. Those values are still much lower then the peaks for the events in Northern Europe, but compared to values for Halloween storms, the values are much higher. The value of 40 A should be safe for the devices of the Czech transmission network when speaking about the immediate effects, that is one should not expect an immediate collapse or damage of these devices, however the effects of the long-term exposure are still not very well studied and at the moment cannot be ruled out. Statistical studies by other authors have already demonstrated the increased rate of anomalies after significant variations of the geomagnetic activity in several countries, including the Czech Republic. These results might be explained by the long-term cumulative effects.

From the results of calculation it is clear, that higher values are expected for bigger substations with more transmission lines and also longer transmission

lines. From the results of geomagnetical voltage calculation, we can see, that higher amplitudes are expected for lines that are longer. The risk of GIC effect could be reduced by splitting transmission lines to shorter transmission lines, as for example was made in 2019 for the V413. Another value, that can reduce the risk of GIC is grounding resistance of the substation, the lower the grounding resistance is, the higher are the expected values of GIC.

Because of the unknown grounding resistances for most of the substations, we had to replace the unknown values by the generic ones to calculate the GICs. We tested the sensitivity of the resulting GIC on the several choices. From the results it is obvious, that the calculated values do not significantly vary with earthing resistance, the differences are in the order of tens of per cents. However, for more accurate GIC calculations, it is necessary to know the accurate values for all substations in the studied system.

Calculated GIC values of were compared to measured values in April 2019 for substation Mírovka, which should had been used to validate the program and model itself. However, the comparison is very inconclusive due to the high-amplitude peaks, the origin of which we do not know. Origin of those peaks could not be GIC, because during this period, the solar activity was very low and the very large values seen in the measurements were not expected.

The main deliverable of my thesis is a universal Python code that allows to model GIC amplitudes for the given network topology and externally given geoelectric field. Both inputs enter the code in a form of external files, which are then automatically processed and the GICs for each of the nodes in network are calculated and stored in the output files. The code also provides plots of both the intermediate and final quantities, such as the geomagnetic voltages for each power line, ideal-earthing currents in each node, and finally the GICs in each node. The modularity of the code allows to apply it to study transmission network of virtually any topology by using geoelectric field provided from any physically relevant models.



Bibliography

- [1] ERU CZ, “Share of electricity production by source,” 2020. [Online; accessed: 09.04.2021].
- [2] Wikipedia contributors, “Geomagnetically induced current,” 2020. [Online; accessed: 12.12.2020].
- [3] Wikipedia contributors, “Solar phenomena,” 2020. [Online; accessed: 12.12.2020].
- [4] Wikipedia contributors, “Geomagnetic storm,” 2020. [Online; accessed: 12.12.2020].
- [5] N. S. W. P. Center, “Coronal mass ejections,” *Coronal Mass Ejections / NOAA / NWS Space Weather Prediction Center*, 2021. [Online; accessed 11-August-2021].
- [6] Wikipedia, “Geomagnetic storm — Wikipedia, the free encyclopedia.” https://en.wikipedia.org/wiki/Geomagnetic_storm, 2021. [Online; accessed 11-August-2021].
- [7] Wikipedia, “Aurora — Wikipedia, the free encyclopedia.” <https://en.wikipedia.org/wiki/Aurora>, 2021. [Online; accessed 11-August-2021].
- [8] Wikipedia, “Maxwell’s equations — Wikipedia, the free encyclopedia.” https://en.wikipedia.org/wiki/Maxwell127s_equations, 2021. [Online; accessed 11-August-2021].
- [9] Jennifer L. Gannon, “Geomagnetic storms and geomagnetically induced currents,” 2016. [Online; accessed: 30.12.2020].
- [10] P. Marketos, A. Moses, and J. Hall, “Effect of dc voltage on ac magnetisation of transformer core steel,” 2010.
- [11] A. Pulkkinen, R. Pirjola, and A. Viljanen, “Statistics of extreme geomagnetically induced current events,” *Space Weather*, vol. 6, pp. n/a–n/a, jul 2008.
- [12] Wikipedia contributors, “Carrington event,” 2020. [Online; accessed: 28.12.2020].

- [13] Wikipedia contributors, “May 1921 geomagnetic storm,” 2020. [Online; accessed: 28.12.2020].
- [14] Solar Storms, “May 13, 1921 – the new york railroad storm,” 2020. [Online; accessed: 28.12.2020].
- [15] Dr. Sten Odenwald, “The day the sun brought darkness,” 2009. [Online; accessed: 30.12.2020].
- [16] Guillon, S., Toner, P., Gibson, L., & Boteler, D., “Colorful blackout: The havoc caused by auroral electrojet generated magnetic field variations in 1989,” 2016. [Online; accessed: 02.06.2021].
- [17] Wikipedia contributorsd, “March 1989 geomagnetic storm,” 2020. [Online; accessed: 30.12.2020].
- [18] Holly Zell, “Halloween storms of 2003 still the scariest,” 2007. [Online; accessed: 30.12.2020].
- [19] Elizabeth Howell, “Giant halloween solar storm sparked earth scares 10 years ago,” 2013. [Online; accessed: 30.12.2020].
- [20] Wik, M., Pirjola, R., Lundstedt, H., Viljanen, A., Wintoft, P., Pulkkinen, A., “Space weather events in july 1982 and october 2003 and the effects of geomagnetically induced currents on swedish technical systems,” 2009. [Online; accessed: 30.12.2020].
- [21] A. Pulkkinen, A. Thomson, C. E., and A. McKay, “April 2000 geomagnetic storm: ionospheric drivers of large geomagnetically induced currents,” 2003. [Online; accessed: 03.06.2021].
- [22] R. L. Bailey, T. S. Halbedl, I. Schattauer, A. Römer, G. Achleitner, C. D. Beggan, V. Wetztergom, R. Egli, and R. Leonhardt, “Modelling geomagnetically induced currents in midlatitude central europe using a thin-sheet approach,” *Annales Geophysicae*, vol. 35, pp. 751–761, June 2017.
- [23] R. Pirjola, “Review On The Calculation Of Surface Electric And Magnetic Fields And Of Geomagnetically Induced Currents In Ground-Based Technological Systems,” *Surveys in Geophysics*, vol. 23, pp. 71–90, Jan. 2002.
- [24] R. L. Bailey, T. S. Halbedl, I. Schattauer, G. Achleitner, and R. Leonhardt, “Validating GIC models with measurements in austria: Evaluation of accuracy and sensitivity to input parameters,” *Space Weather*, vol. 16, pp. 887–902, July 2018.
- [25] R. Tozzi, P. D. Michelis, I. Coco, and F. Giannattasio, “A preliminary risk assessment of geomagnetically induced currents over the italian territory,” *Space Weather*, vol. 17, pp. 46–58, Jan. 2019.

- [26] J. M. Torta, L. Serrano, J. R. Regué, A. M. Sánchez, and E. Roldán, “Geomagnetically induced currents in a power grid of northeastern Spain,” *Space Weather*, vol. 10, pp. n/a–n/a, June 2012.
- [27] P. Hejda and J. Bochníček, “Geomagnetically induced pipe-to-soil voltages in the Czech oil pipelines during October–November 2003,” *Annales Geophysicae*, vol. 23, pp. 3089–3093, Nov. 2005.
- [28] Wikipedia, “Ropovod Ingolstadt – Kralupy nad Vltavou – Litvínov — Wikipedia, the free encyclopedia.” <http://cs.wikipedia.org/w/index.php?title=Ropovod%20Ingolstadt%20%E2%80%93%20Kralupy%20nad%20Vltavou%20%E2%80%93%20Litv%C3%ADnov&oldid=19980715>, 2021. [Online; accessed 18-July-2021].
- [29] T. Výbošt’oková and M. Švanda, “Statistical analysis of the correlation between anomalies in the Czech electric power grid and geomagnetic activity,” *Space Weather*, vol. 17, pp. 1208–1218, Aug. 2019.
- [30] M. Švanda, D. Mourenas, K. Žertová, and T. Výbošt’oková, “Immediate and delayed responses of power lines and transformers in the Czech electric power grid to geomagnetic storms,” *Journal of Space Weather and Space Climate*, vol. 10, p. 26, 2020.
- [31] ČEPS, “Údaje o přenosové soustavě,” 2017. [Online; accessed: 24.4.2019].
- [32] P. Ripka, P. Mlejnek, P. Hejda, A. Chirtsov, and J. Vyhnaněk, “Rectangular array electric current transducer with integrated fluxgate sensors,” *Sensors*, vol. 19, no. 22, 2019.
- [33] P. Hejda, P. Mlejnek, and J. Pek, “Geomagnetically induced currents recorded in the Czech power lines,” in *EGU General Assembly Conference Abstracts*, EGU General Assembly Conference Abstracts, p. 6953, Apr. 2019.
- [34] R. Pirjola, “Geomagnetically induced currents as ground effects of space weather,” in *Space Science*, InTech, Mar 2012.
- [35] GIS, “Souřadnicové systémy,” 2010. [Online; accessed: 30.12.2020].
- [36] T. Výbošt’oková, “Effects of solar activity in power-distribution grids,” Master’s thesis, Astronomical Institute of Charles University, 2019.
- [37] C. Sucksdorff, R. Pirjola, and L. Häkkinen, “Computer production of K-indices based on linear elimination,” *Geophysical transactions*, vol. 36, pp. 333–345, 1991.